

LATE BURIAL TO EARLY TECTONIC QUARTZ VEINS IN THE PERIPHERY OF THE HIGH-ARDENNE SLATE BELT (RURSEE, NORTH EIFEL, GERMANY)

Koen VAN NOTEN^{1,*}, Christoph HILGERS², Janos L. URAI² & Manuel SINTUBIN¹

(14 figures and 1 table)

1. Geodynamics & Geofluids Research Group, Katholieke Universiteit Leuven, Celestijnenlaan 200E, B-3001 Leuven, Belgium; E-mail: koen.vannoten@geo.kuleuven.be, manuel.sintubin@geo.kuleuven.be

2. Geologie-Endogene Dynamik, RWTH Aachen, Lochnerstrasse 4-20, D-52056 Aachen, Germany; E-mail: c.hilgers@ged.rwth-aachen.de, j.urai@ged.rwth-aachen.de

* corresponding author

ABSTRACT. A detailed structural mapping and geometrical analysis of distinct bedding-(sub)perpendicular and bedding-parallel quartz veins has been performed in the northeastern part of the High-Ardenne slate belt (Rursee, North Eifel, Germany), with the aim to reconstruct the local fracturing/veining history. The structural relationship of these two types of veins as well as their relationship with cleavage, folds and faults allows attributing a pre- to early-Variscan age to these veins. The first type of veins is oriented (sub)perpendicular to bedding and consists of several, mutual cross-cutting generations, which clearly predate Variscan deformation. The second type of veins, bedding-parallel veins, post-dates the bedding-(sub)perpendicular veins and reflects bedding-parallel thrusting at the onset of Variscan deformation, predating folding. Subsequently, during progressive Variscan compression both types of veins were passively folded within characteristic, NW-vergent, overturned folds. Locally, due to flexural slip folding, reactivation along the bedding-parallel veins may have taken place.

KEYWORDS: Lower Devonian, Variscides, quartz veining, bedding-parallel thrusting, Eifel.

1. Introduction

The kinematics and composition of syntectonic veins have frequently been studied in orogens (e.g. Urai *et al.*, 1991; Hilgers & Urai, 2002; Schultz *et al.*, 2002). Although early veins, which formed prior to cleavage development, folding or faulting, have an important impact on the paleo-rheology of rock, such pre-tectonic veins have often been neglected in structurally complex systems. If studied carefully, these early veins contain, however, a lot of information concerning the development (e.g. Fitches *et al.*, 1986) and deformation of sedimentary basins (e.g. Kenis, 2004). Furthermore, the regional significance of bedding-parallel veins has often been underestimated. These veins can provide insights into the early structural evolution of fold-and-thrust belts, even though some features are obscured by local reactivation or recrystallisation (Séjourné *et al.*, 2005).

Research in the central part of the High-Ardenne slate belt (HASB) (Bastogne area, Belgium; Fig. 1) revealed that early, pre-folding, fracturing gave rise to a regional occurrence of well-arranged veins in Lower Devonian metasediments (Kenis *et al.*, 2002; Kenis, 2004; Kenis & Sintubin, 2007). This fracturing is exemplified by lenticular, bedding-normal quartz veins organised in parallel arrays, which were formed by the mechanism of hydraulic fracturing (Kenis *et al.*, 2002) in regionally

occurring high fluid pressure compartments during the latest stages of the burial history (Urai *et al.*, 2001; Kenis *et al.*, 2002). Due to the occurrence of high fluid pressures at the time of the veining, the Ardenne-Eifel area can be considered exposing a 340 million year old fractured reservoir (Hilgers *et al.*, 2000; Kenis & Sintubin, 2007). Subsequently, veining was followed by layer-parallel shortening at the onset of Variscan deformation. The early quartz veins acted as mechanical boundaries due to their difference in strength with respect to the psammite and lead to the formation of a cusped-lobate geometry on the pelite-psammite interfaces in between the veins, *i.e.* mullions (Urai *et al.*, 2001; Kenis *et al.*, 2002). This example demonstrates the kinematic impact early veins can play in the subsequent deformation history.

Based on the occurrence of these mullions in the HASB, *e.g.* published in Pilger & Schmidt (1957), Sippli (1981), Spaeth (1986) and Kenis *et al.* (2002), two different areas can be distinguished: a central part where mullions are present and a peripheral part where they are mostly absent (Figs 1 & 2). Contrary to the regionally well-arranged vein-set in the central part, quartz veining is less consistent in orientation in the periphery. The occurrence of numerous quartz vein generations with mutual cross-cutting relationships indicates a more complex fracturing/veining history than in the central part. Furthermore, the absence of mullions associated

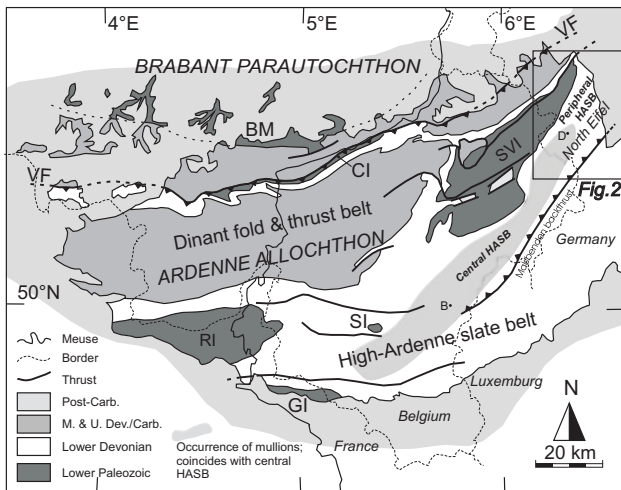


Figure 1: Geological map of the Ardenne-Eifel area (France, Belgium, Luxembourg and Germany). The occurrence of mullions in the High-Ardenne slate belt (HASB), coinciding with the central HASB, and the periphery of the HASB in the North Eifel are indicated. VF = Variscan Front Zone, i.e. Aachen/Midi Fault; BM = Brabant Massif; CI = Condroz Inlier; RI = Rocroi Inlier; SI = Serpont Inlier; GI = Givonne Inlier; SVI = Stavelot-Venn Inlier; B = Bastogne; D = Dedenborn.

with pre-tectonic quartz veins suggests that incipient Variscan shortening is expressed differently in the peripheral part.

This paper documents on an analysis of the overall structural architecture and all related structural features which are observed around the Rursee water reservoir (30 km ESE from Aachen; Fig. 2). The excellent degree of exposure is an opportunity to focus on the characteristics of quartz veining in the peripheral part of the HASB. A considerable effort has been put in the analysis of the orientation and characteristics of the omnipresent bedding-(sub)perpendicular quartz veins in order to set up a paragenesis of the different cross-cutting vein generations. This paragenesis allows us to reconstruct the complex fracturing/veining history in the periphery of the HASB. Furthermore, we also focus on the formation of bedding-parallel quartz veins in order to reveal the early structural evolution of the area. Finally, we briefly discuss the differences in veining between the central and the peripheral part of the slate belt, wondering how similar geodynamic constraints are expressed differently at different structural levels in a developing slate belt.

2. Geological Setting

2.1. Ardenne-Eifel area

In the Ardenne-Eifel area (France, Belgium, Luxembourg, Germany; Fig. 1) the northern extremity of the Central European Variscides, the so-called Rhenohercynian foreland fold-and-thrust belt (Oncken *et al.*, 1999), is cropping out. The northern frontal parts of the fold-and-thrust belt are characterised by the presence of a major

allochthonous domain, the Ardenne allochthon, which thrust over its foreland, the Brabant parautochthon during the latest – Asturian – stage of the Variscan orogeny (late Carboniferous) (Meilliez & Mansy, 1990; Mansy & Lacquement, 2003). The Ardenne allochthon can be subdivided in the Dinant fold-and-thrust belt, in which the deformation is mainly controlled by a competent Devonian-Carboniferous sedimentary sequence (Meilliez & Mansy, 1990; Lacquement, 2001), and the High-Ardenne slate belt, in which a slaty cleavage is the dominant structural feature. This slate belt consists of Lower Devonian siliciclastic, predominantly argillaceous sequences, which underwent a very low- (anchizonal) to low-grade (epizonal) metamorphism, which is considered to have a burial origin and is believed to be pre- to early synkinematic with respect to the prograding Variscan deformation (Fielitz & Mansy, 1999).

2.2. North Eifel stratigraphy

The Rursee is located in the German part of the HASB (Fig. 1). The latter area is bordered by the Stavelot-Venn Inlier in the NW, by the Malsbenden backthrust in the SE and is covered by subhorizontal Triassic deposits in the East (Figs 1 & 2). The NNE-SSW-trending Lower Devonian metasedimentary rocks rest unconformably on the SE-dipping limb of the NE-plunging Lower Paleozoic Stavelot-Venn Inlier (see cross-sections on Fig. 2). The rapid syn-rift Ardenne-Eifel basin fill on the northern passive continental margin of the developing Rhenohercynian Ocean (Oncken *et al.*, 1999), particularly active during the Pragian, is now comprised in the High-Ardenne slate belt as thick Lower Devonian sequences. Due to the northwards transgression, metasediments in the North Eifel are diachronous with respect to metasediments in the High-Ardenne (Goemaere & Dejonghe, 2005). They progressively young up from the central part of the HASB towards the periphery, evolving from a Lochkovian-Pragian to a Pragian-Emsian age respectively.

The sequences in the Rursee area all belong to the Upper Rurberg and Heimbach beds (Wünstorf, 1931, 1936, 1943; Ribbert, 1992). The Rurberg beds are characterised by dark blue mudstones and differ from the underlying Monschau beds, which mainly contain sandstone beds. Stratigraphically, the Rurberg beds are divided in three different units in which the content of sandy material increases from the Lower-, over the Middle-, towards the Upper Rurberg beds (Fig. 2). Stratigraphic borders in between the units are rather vague since units are gradually changing into each other. The Upper Rurberg beds belong to the upper Pragian and expose an alternation of predominantly mudstones with silt- and fine-grained sandstones intercalated with thick coarse-grained sandstones. Estimation of the thickness of these Upper Rurberg beds is difficult due to the diachronous nature and due to synsedimentary faulting (Oncken *et al.*, 1999) in the subsiding Lower Devonian Ardenne-Eifel basin. Thickness changes laterally from 600 m to 2000 m in the North Eifel and varies around 1000 m in the Rur

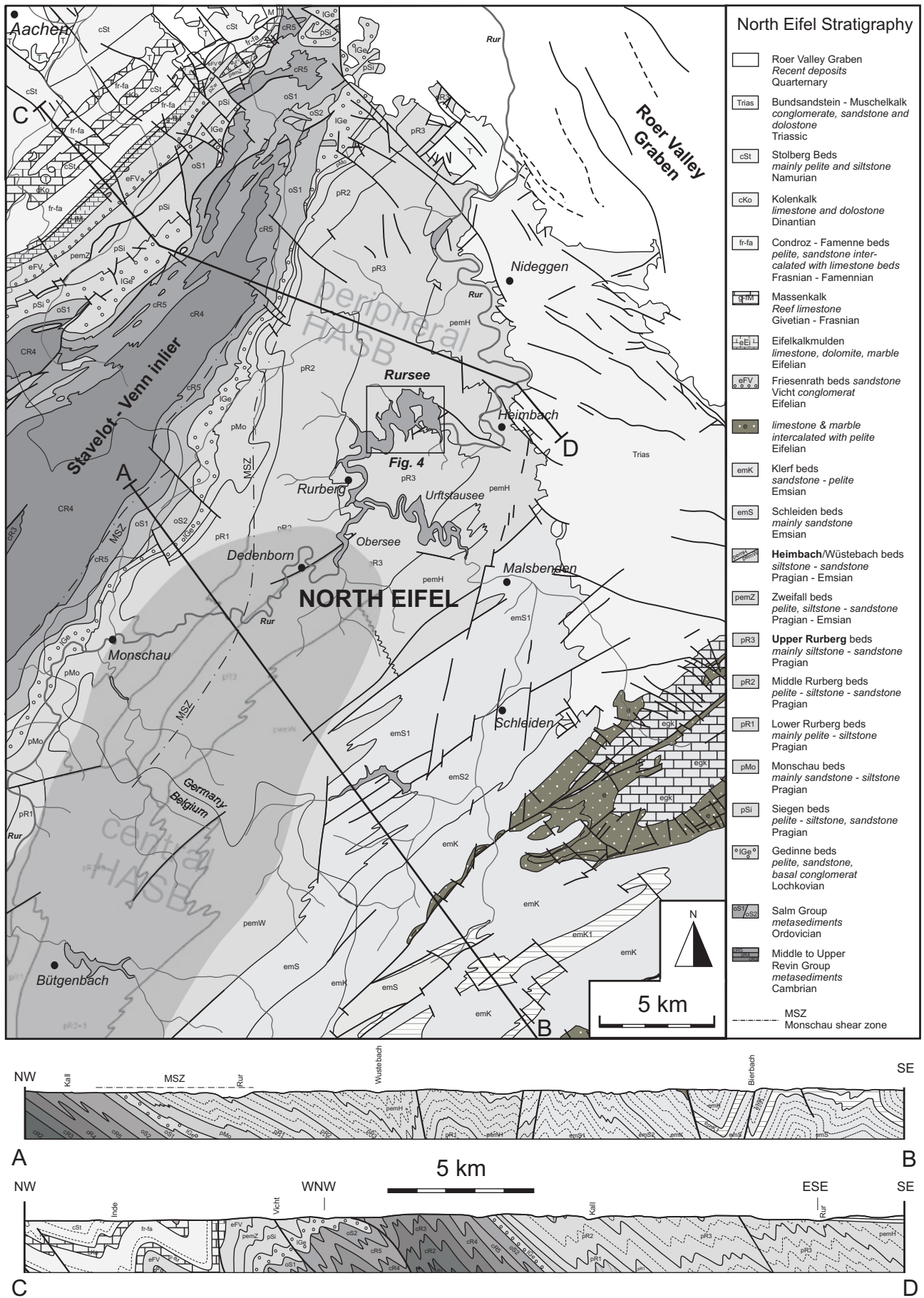


Figure 2: Lithostratigraphic map of the North Eifel, bordered by the Stavelot-Venn Inlier in the West and the Triassic cover in the East (modified after Ribbert, 1992). See legend and text for description of the lithostratigraphic units. Besides Dedenborn, type locality of the mullions, also other towns are indicated. The occurrence of mullions is indicated in grey.

valley (Richter, 1967; Knapp, 1980; von Winterfeld, 1994).

Towards the East, the Upper Rurberg beds gradually change into the younger Heimbach beds (Wünstorf, 1936; Fig. 2), which have an upper Pragian to lower Emsian age (biozonation in Richter, 1967 and references herein). The Heimbach beds are characterised by grey-blue mudstones intercalated with thin sandstone beds. Thickness varies up to 500 m, although this estimation is highly uncertain because of the unknown fault throw of the Malsbenden backthrust in the SE and because of the overlying Triassic deposits in the East (Richter, 1967; Knapp, 1980). Although Ribbert (1992) made a clear distinction between the Upper Rurberg and the overlying Heimbach beds in the SE of the study area (Fig. 2), it is impossible to recognise a lithostratigraphic border between both units in the field.

2.3. Variscan deformation in the North Eifel

The metasediments in the North Eifel, with the exception of those in the epizonal Monschau shear zone (Fig. 2), only suffered an anchizonal metamorphism (see metamorphic zonation in Fielitz & Mansy, 1999). Deformation temperatures were at the lowermost boundary of quartz recrystallisation and did not exceed 300°C (von Winterfeld, 1994).

The late Carboniferous Variscan shortening of the Rhenohercynian belt created different fold styles in the North Eifel. Folds gradually vary from hectometre-scale, upright folds in the Malsbenden-Schleiden area in the SE (Fig. 2; SE of cross-section A-B), into overturned, NW-verging folds in the Rursee and surrounding areas (Fig. 2;

NW of cross-section A-B and SE of cross-section C-D). Towards the SW-border of the Stavelot-Venn Inlier, small-scale minor folds characterise the Monschau shear zone. The latter contains NNW-verging, East-plunging folds (Spaeth, 1979; Fielitz, 1992), a trend which differs distinctly from the general NE-SW trend of the major hectometre folds in the Rhenish Massif. Concomitant with these varying fold styles, an increase of slaty cleavage development exists from the SE towards the NW of the North Eifel. Moreover, cleavage gradually varies from an almost vertical spaced cleavage in the Malsbenden-Schleiden area towards a gently inclined (30° SE) slaty or continuous cleavage in the intensely deformed and metamorphosed SE-limb of the Stavelot-Venn Inlier (Wünstorf, 1934; Hoffmann, 1961). Deformation thus increases towards the NW. The North Eifel is furthermore characterised by SE-dipping faults and thrusts, of which some faults are interpreted as inverted, pre-shortening synsedimentary faults (Oncken *et al.*, 1999).

The overall structural architecture of the High-Ardenne slate belt changes from NW-verging, NE-SW-trending fold trains in the North Eifel (Germany) into upright, slightly North-verging, East-West-trending folds near Bastogne (see Fig. 4 in Hance *et al.*, 1999). Also the dominant, pervasive slaty cleavage in the slate belt changes from moderately SE-dipping to steeply S-dipping respectively. According to Fielitz (1992), this change in structural fold style is probably related to the southern border of the pre-Variscan subsurface basement high in the foreland, the Anglo-Brabant Deformation Belt.

The Late Carboniferous Variscan deformation was followed by a long period of tectonic quiescence during



Figure 3: Characteristic lithologies, sedimentological features and examples of small-scale soft-sediment deformation. See Fig. 4 for location. A) Relatively undisturbed, overturned Heimbach beds, as indicated by a bedding dipping steeper than cleavage, younging towards the N (shown by arrow). Cleavage (S_1) shows a sharp refraction at the siltstone - sandstone interface (left) and changes gradually in orientation towards the slaty units (right) into a slaty cleavage (zone 13 on Fig. 4). B) Normal, SE-dipping Rurberg beds showing an intercalation of cross-laminated coarse-grained sediments and a gully filled up with wavy, parallel laminated silty sediments (m175, zone 8 on Fig. 6). C) Ripple marks visible on an overturned bedding plane of a Heimbach sandstone bed (zone 13 on Fig. 4). D) Shortened load-casts (m55, zone 5 on Fig. 6.). E) Heimbach beds with reverse structural and stratigraphic polarity showing large-scale point bars and an alteration of silt- and sandstone beds (zone 13 on Fig. 4).

Mesozoic, followed by uplift (doming), erosion and post-orogenic faulting. Uplift of the Ardennes - Rhenish Massif started in the Upper Cretaceous. Major doming started in the late Oligocene and continued until recent times (Walter, 1992; Garcia-Castellanos *et al.*, 2000).

3. Lithology and sedimentology

The studied sequences in the eastern part of the Rursee area are present in excellent outcrops along the hiking path and are continuous over several hundred of metres along the shores around the water reservoir. Due to seasonal water level fluctuations (> 10 m), outcrops at the shores are free of any surface weathering.

Most outcrops consist of an alternation of predominantly clayey-silty sequences and decimetre- to metre-scale thick coarse-grained sandstones (Fig. 3A). An energetic depositional environment is suggested by the occurrence of small-scale sedimentary structures such as ripple marks, cross-beds, wavy parallel laminations and cross-laminations (Figs 3B & C). The more energetically deposited, coarse-grained beds are characterised by small

centimetre- to decimetre-scale channels (gullies), which are filled up with laminated to cross-bedded sandy sediments and are separated from each other by thin, millimetric pelitic lamellae. Large-scale structures, such as point bars, are represented by coarse-grained beds, which wedge out after a few decametres (Fig. 3D). Apart from these sedimentary structures, small-scale synsedimentary deformations such as convolutions and load-casts occur. Load-casts, present at the competent-incompetent interface (Fig. 3E), are useful to determine the stratigraphic polarity. Throughout the mudstone-siltstone-sandstone sequences, a coarsening upwards is sometimes observed and is expressed by the pervasive cleavage, which gradually changes in orientation from a slaty cleavage in the incompetent sediments towards a spaced cleavage in the competent beds (Fig. 3A). At the top of the sequences cleavage refracts at high angles to the competent-incompetent (sandstone - pelite) interface.

The above described sedimentological features give evidence for a shallow marine, deltaic to tidal depositional environment on the northern shelf of the rapidly subsiding Rhenohercynian basin.

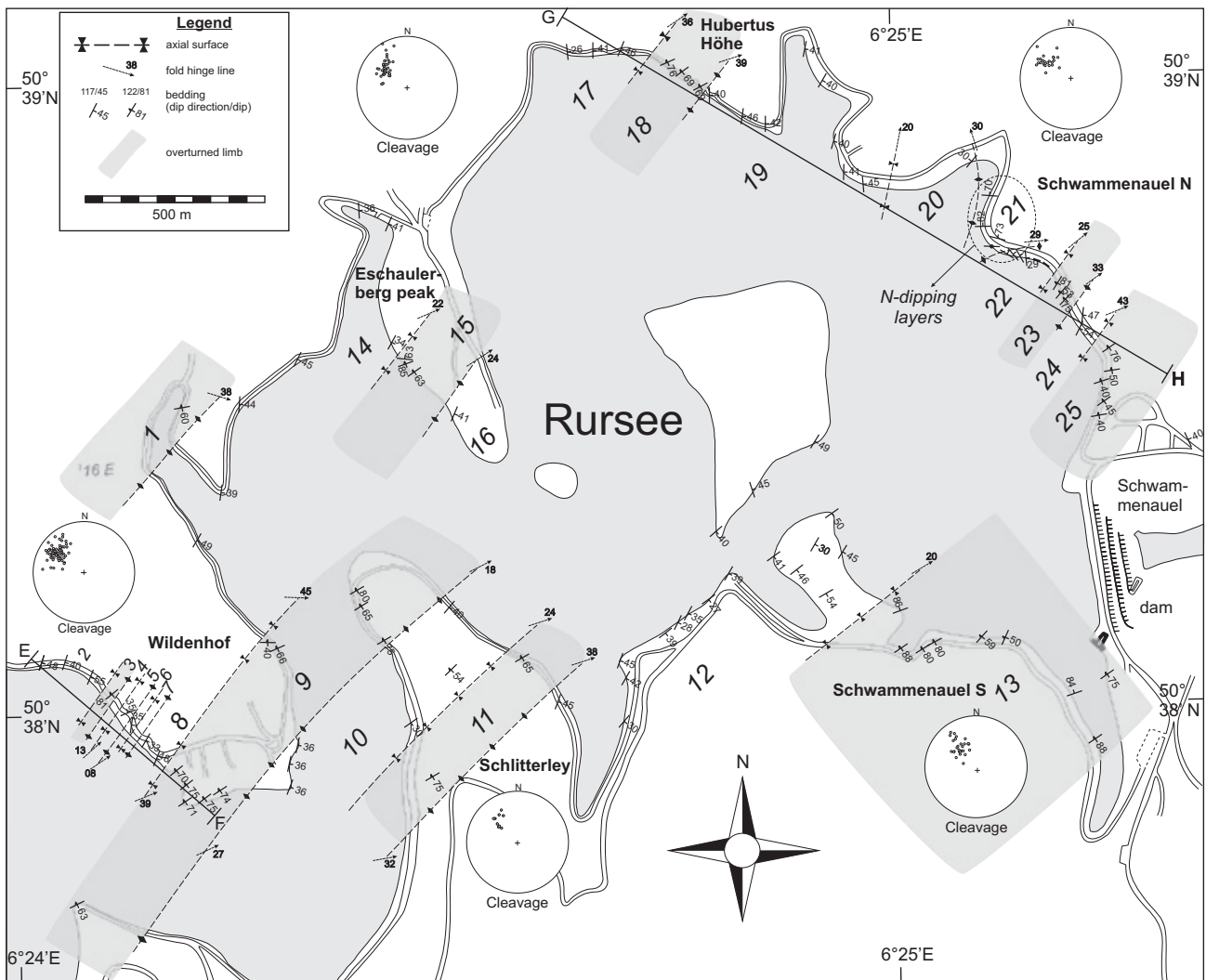


Figure 4: Structural map of the Rursee area with cross-section E-F (Wildenhof ; Fig. 6) in the SW-part and cross-section G-H (Hubertus-Höhe - Schwammenauel N ; Fig. 8) in the NE-part of the area. The outcrops in the NE of the map are situated on a higher structural and stratigraphic level. See text for discussion. See Table 1 for the specific field data of zones 1-25.

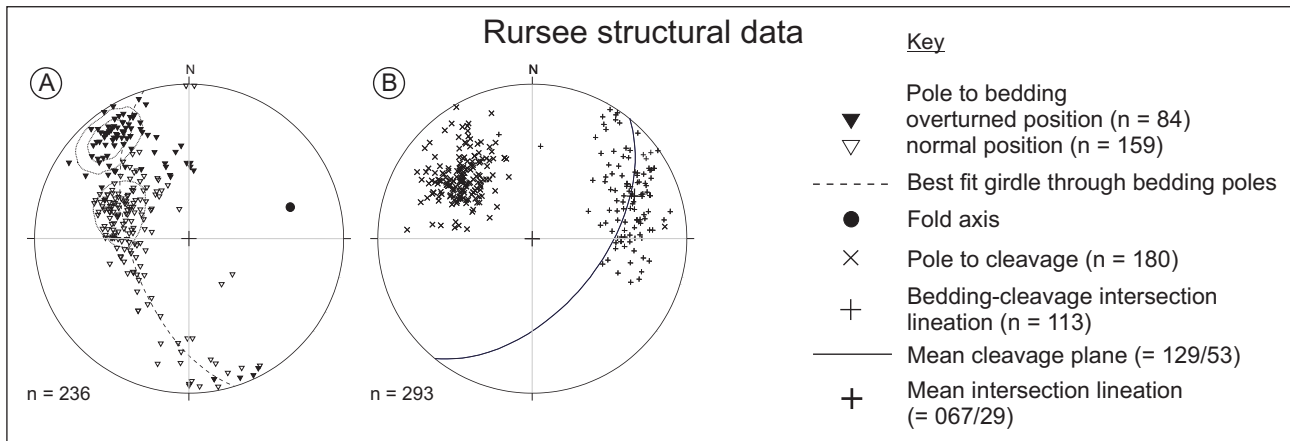


Figure 5: Lower-hemisphere, equal-area projections showing the orientation of bedding (A; contour lines of 16% and 32%) and cleavage and bedding-cleavage intersection lineation (B).

4. Structural analysis

In order to frame veining, we first need to understand the overall architecture of the study area. The data in this section include the geometry of structural features such as bedding, cleavage, bedding-cleavage intersection lineation and fold hinge line. The fold hinge line is the line measured at the fold hinge, while the fold axis is the constructed intersection of two fold limbs on the stereographic projection and thus cannot be measured in the field. These field observations are summarised in Table 1. The orientation of planar features (bedding, cleavage) is written as dip direction/dip (*e.g.* 045/85 for a plane dipping 85° to the NE) and the orientation of linear features (intersections, fold hinge lines) is written as trend/plunge (*e.g.* 045/85 for a line plunging 85° to the NE). Throughout the description the data are mostly the mean values of several measurements, unless specifically mentioned.

4.1. Overall structural architecture

The overall structural architecture is very consistent (Fig. 4) and displays first order, asymmetric to overturned, hectometre-scale folds with close interlimb angles and with a NW-verging asymmetry. The overturned folds have rounded to angular fold hinges. Stereographic analysis of bedding (Fig. 5A) shows that the folds are highly cylindrical. Two separate clusters, representing limbs with a normal (113/41) and an overturned (143/69) structural polarity, can clearly be recognised.

The main tectonic foliation is a distinct pervasive cleavage of which the attitude remains constant throughout the whole study area (129/53). Whereas the incompetent rocks (*i.e.* pelite and siltstone) are characterised by a slaty cleavage, a weak or spaced cleavage exists in the competent sandstone beds. The stereographic projection of cleavage (Fig. 5B) indicates that cleavage is axial planar with respect to the folds.

The bedding-cleavage intersection lineation is the most prominent linear feature and can be used as a tool to predict the orientation of the local fold hinge line. The intersection lineation varies from gently to steeply NE- to

East-plunging (Fig. 5B). The considerable variability of the bedding-cleavage intersection lineation can be explained by two phenomena: i) Due to irregular sedimentology (*i.e.* large-scale point bars or small-scale gullies) bedding surfaces are rather wavy, while the cleavage attitude remains constant. Because of this, the bedding-cleavage intersection lineation may differ from outcrop to outcrop. ii) Folds die out from the SW to the NE (see fold axes on Fig. 4). Outcrops in the Hubertus-Höhe - Schwammenauel N section (see 4.3.) are therefore situated at a higher structural and stratigraphic level than the outcrops in the Wildenhof section (see 4.2.). Since folds probably have a periclinal nature, with periclinal endings to the NE, fold hinges will slightly differ in orientation in between both sections and hence cannot be interconnected.

4.2. Wildenhof-section (Wildenhof – Schlitterley)

The largest outcrops in the SW of the study area are situated along the NW-SE trending road section at Wildenhof and along the shores of the Wildenhof campsites (Fig. 6). The outcrops beneath the road section, of which the accessibility is highly dependent on the seasonally fluctuating water level, provide a nice correlation with the structures along the road section. The exact position of the discussed outcrops in the text is indicated on the scale-bar below the cross-section in Fig. 6.

For over 450 m, outcrops show syn-cleavage, overturned folds, with a marked NW-verging asymmetry, subangular to rounded hinges and moderately SE-dipping (50° to 60°) axial surfaces. Axial surfaces are exemplified by a pronounced axial planar cleavage, with opposing senses of cleavage refraction in normal SE-dipping limbs (zones 2, 4, 6 & 8) and normal NW- (zones 5 & 7) or overturned SE-dipping (zones 3 & 9) fold limbs. A few outcrops show a local subparallelism of cleavage and bedding (m200, zone 8; zone 13). In some cases local thrusts cross-cut fold hinges, *e.g.* the syncline-anticline couple in between m108 and m115 (Figs 6 & 7A). The latter structure is supposed to have formed along out-of-

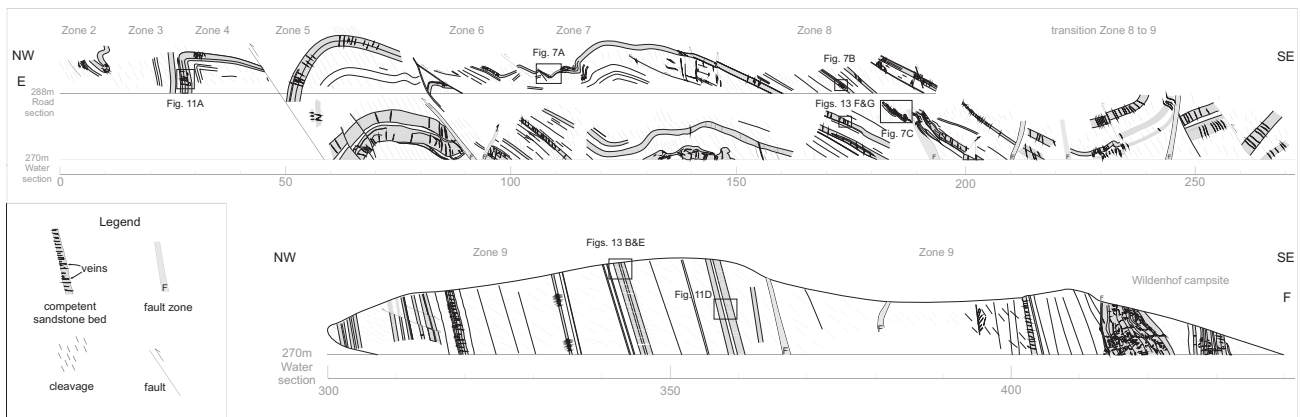


Figure 6 : Wildenhof structural cross-section, constructed by means of photographs, showing bedding, cleavage, faults and veins. The cross-section shows a hectometre-scale sequence comprising NW-verging, upright to overturned, cylindrical folds. Meso-scale folds are only observed near hinges or faults. Cleavage remains SE-dipping throughout the section and is approximately axial planar with respect to the overturned folds. See text for discussion. A gap of 40 m (m260 - m300) exists in between both cross-sections. Note: The upper and lower cross-sections have a different scale.

syncline thrusts. These syn- to late-folding out-of-syncline faults cross-cut the bedding and are characterised by centimetre thick quartz veins. The veins are marked by slickenlines, presumably tracking the out-of-syncline fault movement. The slates just below the synclinal hinge are characterised by a well developed cleavage, which gradually changes from gently dipping just below the hinge zone (Fig. 7A) into its common, moderately SE-dipping orientation. Going from the road level to the water level (m125), this complex syncline-anticline-syncline evolves into a single open syncline (Fig. 6).

Locally, decimetre-scale bed-on-bed movements are observed, representing a top-to-northwest bedding-parallel displacement due to flexural slip folding. The amount of displacement can sometimes be measured by means of displaced (sub)bedding-perpendicular quartz veins (Fig. 7B). The movement horizons or slip planes are localised in thin pelitic layers, which separate the competent sandstone beds.

Between m50 and m100 of the cross-section, two major thrusts are present. The absence of any correlation between beds below and above the thrusts suggests that both faults must have displacements of at least a few tens of metres. The orientation of the moderately to steeply SE-dipping thrusts is largely parallel with the orientation of the axial surfaces of the overturned folds. Also other small-scale thrusts have similar SE-dipping orientations (Fig. 7C). The relative timing of this thrusting remains to be determined, either syn-folding (*i.e.* fault-bend-folding or fault-propagation-folding, *e.g.* Dittmar *et al.*, 1994) or post-folding (break-thrust folding).

At m90, a NW-dipping fault occurs antithetic to the above described thrust. Both faults seem to be genetically related and can be interpreted as a pop-up structure. Another pop-up structure occurs at m200. In contrast to the structure at m90, the displacement along the NW-dipping fault at m200 is observed and measures one metre. Opposite to the latter fault, several small-scale faults at m190 cross-cut the SE-dipping competent beds (*e.g.* two

small-scale, reverse faults, filled up with quartz, displacing a folded sandstone layer over a couple of decimetres; Fig. 7C). The S-shaped smaller-scale fold (Fig. 7C) has a NW-verging asymmetry and is developed on the SE-limb of an anticline. The cross-cutting faults seem highly related to the folding of this SE-dipping layer, due to their comparable NW-directed displacement. A 0.5 m wide, steeply SE-dipping fault zone cuts a hinge of this smaller-scale folded layer at m190 and is characterised by a clayey fault gouge. The exact fault displacement has not been determined.

Similar wide fault zones with associated fault gouges and unknown fault displacements have also been recognised between m200 and m260 where they cross-cut a wide synclinal hinge zone. It remains unclear whether these cross-cutting fault zones have a reverse or normal fault displacement. This wide syncline forms a transition from the mainly, gently SE-dipping layers (m0 to m250) into layers with an overturned polarity, which crop out at the Wildenhof campsite (m300 to m430). This overturned limb shows SE-dipping beds with a mean orientation of 137/73. Cleavage dips less steeply than bedding (128/54), which is indicative for the overturned orientation. Locally at m315, two reverse faults cut the beds with a small displacement. At m420 a sequence of coarse-grained sandstones is densely fractured. The omnipresent siltstones and slates are interrupted by coarse-grained sandstones, mostly characterised by the occurrence of numerous quartz veins. Early bedding-perpendicular veins (5.1.) as well as bedding-parallel veins (5.2.) can be recognised. Apart from these common veins, also irregular veins are present, indicative of local fluid release along small-scale faults. The irregular sedimentology of the layers (*e.g.* point bars) could have been serving as a focus to initiate these faults. The top of this complex zone is bordered by a bedding-parallel fault zone.

The southern overturned limb at Wildenhof (zone 9) can be connected with the northern extremity of the Schlitterley promontory across the Rursee (Fig. 4). Hence,

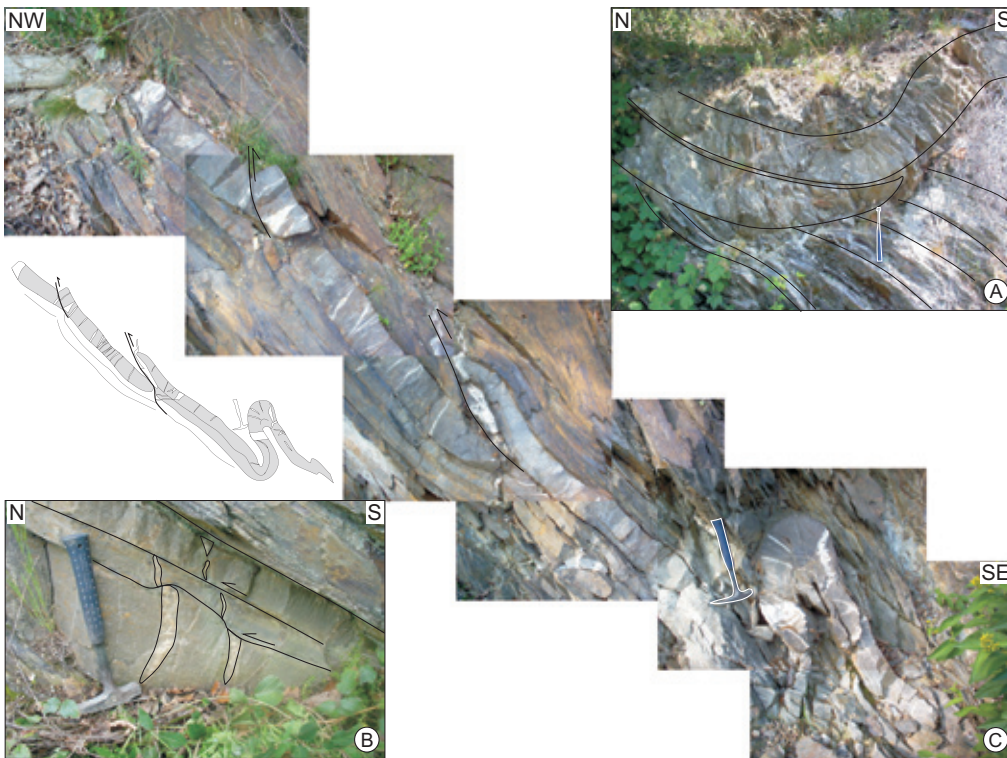


Figure 7 : Examples of deformation structures in the Wildenhof cross-section. See Fig. 4 for location. See hammer for scale (~ 32 cm). A) Out-of-syncline structure (m110, zone 7 on Fig. 4). B) Bed to bed displacements, visualised by displaced bedding-perpendicular quartz veins. The displacement is in agreement with the mechanism of flexural slip in which slip occurred in the thin pelitic layers (m175, zone 8 on Fig. 4). C) Small-scale folded sandstone layer with a NW-verging asymmetry and associated small-scale reverse faults (m185, zone 8 on Fig. 4).

the NW-SE trending Wildenhof fold train, described in this section, continues at Schlitterley towards the SE.

4.3. Hubertus Höhe – Schwammenauel N section

The outcrops along the NW-SE trending road section of the Hubertus Höhe section, which are situated on a higher structural level than the Wildenhof section (4.2.), comprise

similar overturned folds with an associated axial planar cleavage as the Wildenhof section (Figs 1 & 8 and Table 1). Mean cleavage attitude (129/53) is highly comparable with that at Wildenhof (126/55). The East-dipping normal limb (093/41) of zone 19 in the Hubertus-Höhe section, remains constant for over 600 m, suggesting that fold limbs are slightly longer than in the SW of the study area. Eastwards of this limb, bedding changes from East-

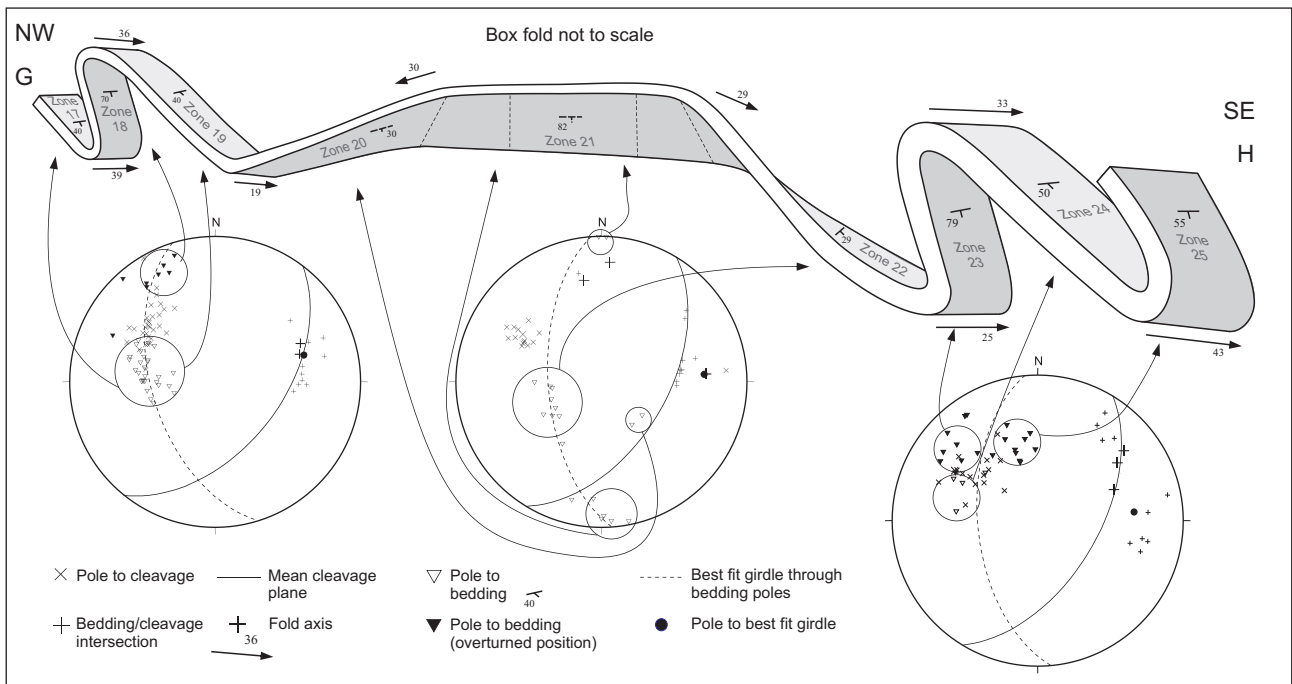


Figure 8: Schematic representation of the fold geometry in between Hubertus Höhe and Schwammenauel N. See Fig. 4 for location. Note that figure is not to scale, but is meant to fit the structure of the box fold into the regional fold style. For true dimensions of the North-dipping layers see Fig. 4. Total length of the cross-section is approximately 2 km. Lower-hemisphere, equal-area projections with structural data are related to each fold style. See text for discussion on the transition between the common overturned folds and the North-plunging box fold.

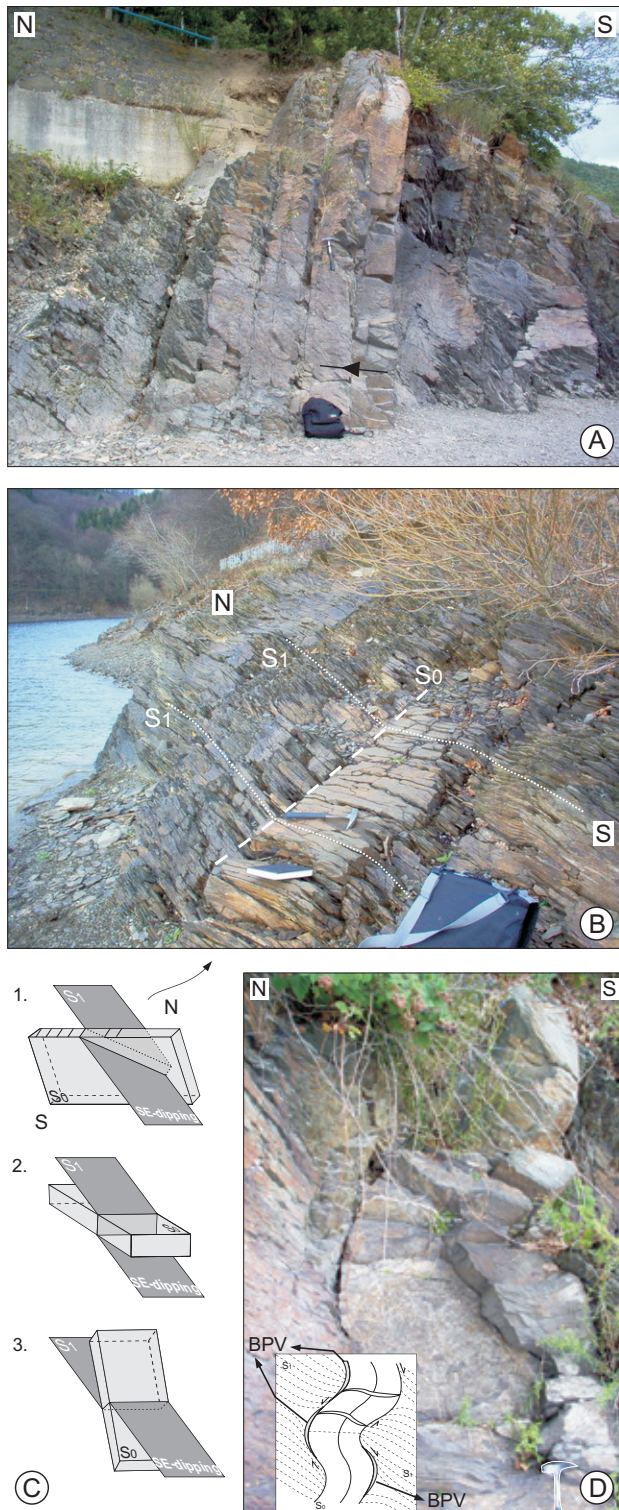


Figure 9: Small-scale observations in the North-dipping layers of the Schwammenauel N outcrops (zone 21). See Fig. 4 for location. A) Photograph of upright, competent North-dipping layers, younging towards the N (shown by arrow). B) Photograph of the 'oblique' cleavage refraction in the North-dipping layers. C) Sketches of different cleavage refraction patterns observed in the different fold styles; 1. 'Oblique' cleavage refraction (cf. Fig. 9B; box fold). 2. Cleavage (S_1) dipping steeper than bedding (S_0) (normal limbs). 3. S_0 dipping steeper than S_1 (overturned limbs). D) Photograph and sketch of the buckled North-dipping layers. Bedding-parallel veins (BPV) occur in the hinges as well as in the cusps of the buckle folds, indicating that BPVs developed before buckling.

dipping to NW-dipping (318/30; zone 20). Also cleavage changes remarkably from SE-dipping (130/50; zone 19) to West-dipping (265/75; zone 20). Cleavage refraction is opposite in both zones, suggesting a synclinal hinge in between. Further to the SE, outcrops suddenly comprise steep, almost upright, buckled, North-dipping layers (000/83; zone 21), younging to the North (Fig. 9A). The latter attitude is found nowhere else in the whole study area. Moreover, this attitude does not fit into the model of the regionally observed overturned folds, in which normal and overturned limbs usually dip to the East and to the SE respectively (see Fig. 5). The upright, North-dipping layers continue over 100 m to the SE, before bending into gently NE-dipping layers (064/32; zone 22). From this normal NE-dipping limb towards the Schwammenauel dam, two more hectometre-scale overturned folds are exposed (zones 23 - 25).

Along the Hubertus Höhe – Schwammenauel N section a transition between two fold styles thus occurs (see Fig. 8 for interpretation). The NW-verging overturned folds, observed at Hubertus Höhe and near the Schwammenauel dam, are interrupted by NW-dipping layers and by the upright, North-dipping layers. The latter two observations give evidence for a box fold with a flat upright hinge zone, *i.e.* the North-dipping layers. Only one of the two fold axes of this box fold is observed (085/39) and corresponds with the layers bending from North-dipping to NE-dipping at the transition of zones 21 - 22. The other fold axis can be deduced by using the bedding-cleavage intersection lineation (342/30) of the NW-dipping layers (zone 20). It is likely that this box fold will die out towards the South. Surprisingly, cleavage in the North-dipping layers dips to the SE (118/51) and remains axial planar with respect to the regional folds, indicating that the formation of this box fold did not influence the regional cleavage attitude. The local bedding-cleavage intersection lineation (085/36) in the North-dipping limb remains parallel with the intersection observed in other outcrops along the Hubertus Höhe – Schwammenauel N section, but varies strongly across the fold hinges of this box fold, suggesting that cleavage developed contemporaneous with folding.

4.4. Kinematic interpretation & discussion

Along the Wildenhof section a transition of smaller-scale folds (zones 2 – 8) with a large overturned fold limb (zone 9) can be observed. The common overturned fold style is also observed along the Schlitterley and Hubertus-Höhe sections and near the Schwammenauel dam. Locally, at Schwammenauel N a transition in fold styles occurs. The origin of the North-dipping attitude of the beds, however, remains unclear. Small-scale observations (Fig. 9), which are summarised below, suggest that tilting of the layers towards the North predates buckling of the competent beds and occurred prior or early during (*e.g.* incipient development of periclinal folds) the pervasive fold-and-cleavage development. Fig. 10 sketches the evolution of the particular deformation structures in the North-dipping layers.

Outcrop	Bedding (S ₀)	β - axis of bedding	Cleavage (S ₁)	S ₀ /S ₁ Li (measured)	S ₀ /S ₁ Li (merged)
Outcrops Wildenhof - Schlitterley:					
zone 1 - 12					
Zone 1	170/60 (2)	-	160/40 (1)	-	085/08 (3)
Zone 2	106/43 (18)	057/32	122/54 (15)	067/39 (4)	049/26 (33)
Zone 3	139/75 (4)	063/42	120/67 (4)	-	052/63 (8)
Zone 4	133/45 (2)	-	145/65 (1)	-	-
Zone 5	346/70 (6)	061/36	138/62 (2)	045/45 (1)	052/49 (8)
Zone 6	069/32 (17)	090/30	119/55 (15)	060/30 (1)	064/34 (32)
Zone 7	145/90 (1)	-	-	-	-
Zone 8	118/39 (12)	-	126/54 (8)	058/30 (3)	-
Zone 9 - Wildenhof	137/73 (51)	220/35	128/54 (24)	060/22 (3)	062/23 (46)
Zone 9 - Schlitterley	149/73 (4)	-	133/45 (3)	068/20 (2)	066/20 (7)
Zone 10 - Wildenhof	104/40 (5)	028/12	140/57 (10)	077/29 (3)	075/35 (15)
Zone 10 - Schlitterley	138/35 (2)	-	152/60 (1)	080/27 (1)	069/14 (3)
Zone 11	150/70 (2)	-	130/40 (2)	073/34 (2)	067/20 (4)
Zone 12	125/32 (18)	-	143/47 (9)	067/19 (6)	058/12 (27)
Zone 1 - 10	Best fit girdle:				
Wildenhof fold train	248/58 (84)	068/32	126/55 (75)	066/32 (13)	066/33 (159)
Zone 9 - 12	Best fit girdle:				
Schlitterley fold train	247/70 (9)	067/20	139/46 (7)	072/27 (5)	068/20 (16)
Outcrops Eschaulerberg peak: zone 14 - 16					
Zone 14	106/38 (6)	-	121/45 (5)	062/24 (1)	081/35 (10)
Zone 14 - 15: transition	001/65 (3)	-	137/62 (3)	-	075/23 (6)
Zone 15	144/68 (4)	-	132/43 (4)	069/25 (1)	067/23 (8)
Zone 16	100/41 (1)	-	127/64 (1)	090/44 (1)	054/31 (2)
Zone 14 - 16	Best fit girdle:				
Esch. fold train	252/57 (14)	072/33	133/48 (13)	072/32 (3)	074/31 (27)
Outcrops Hubertus Höhe: zone 17 - 20					
Zone 17	103/38 (11)	039/19	131/52 (9)	066/27 (3)	064/30 (20)
Zone 18	148/72 (9)	-	126/47 (8)	075/36 (2)	073/34 (17)
Zone 19	093/41 (18)	078/40	130/50 (12)	093/42 (6)	087/40 (30)
Zone 17 - 19	Best fit girdle:				
H. H. fold train	252/53 (39)	072/37	130/50 (29)	082/32 (11)	076/37 (68)
Outcrops Schwammenauel N: zone 21-25					
Zone 20 NW-dipping	318/30 (2)	317/30	265/75 ! (1)	342/30 (1)	347/27 (3)
Zone 21 N-dipping	000/83 (8)	085/39	118/51 (6)	085/36 (6)	083/45 (14)
Zone 22 NE-dipping	064/32 (9)	077/31	128/58 (5)	082/30 (1)	060/31 (14)
Zone 23	128/64 (7)	-	126/44 (6)	036/21 (3)	-
Zone 24	123/47 (4)	113/47	116/58 (2)	039/30 (1)	128/51 (6)
Zone 25	160/48 (12)	-	136/42 (6)	096/25 (6)	078/15 (18)
Zone 21 - 25	Best fit girdle:				
Schw. N fold train	265/57 (41)	085/33	125/49 (25)	077/32 (17)	083/36 (66)
Outcrops Schwammenauel S: zone 12-13					
Zone 13	147/75 (19)	069/37	136/47 (12)	063/23 (11)	066/25 (31)
Zone 12 - 13: transition	336/86 (2)	-	147/77 (2)	070/20 (1)	064/28 (4)
Zone 12 - Schwam S	129/38 (38)	080/27	147/47 (17)	076/24 (13)	081/27 (55)
Zone 12 - 13	Best fit girdle:				
Schw S. fold train	246/69 (59)	066/21	142/50 (31)	070/24 (25)	067/20 (90)

Table 1: Bedding and cleavage data in the investigated zones. See Fig. 4 for location of zones. The orientation of planar features (bedding: S₀, cleavage: S₁) is written as dip direction/dip and the orientation of linear features (fold hinge lines; S₀/S₁ intersection lineation: Li) is written as plunge direction/plunge. The number of measurements is given in between brackets. Entries in bold correspond with exceptional data found nowhere else in the study area. Grey zones represent data of the overturned limbs. The bedding-cleavage intersection lineations are measured in the field (column 5) and calculated by merging bedding and cleavage data (column 6). (-): not observed or suspicious data.

Firstly, cleavage does not refract as one would expect in the normal or overturned limbs, but rather refracts ‘obliquely’ through the competent layers (see Figs 9B & C). Generally, onset of cleavage development is assumed to occur during layer-parallel shortening prior to folding (Treagus, 1983). With ongoing shortening pelite and sandstone will behave differently and sandstone will start to buckle. The embryonic cleavage within the sandstone layers will rotate passively during buckling, which

eventually leads to cleavage refraction (Treagus, 1983; Van Baelen & Sintubin, 2008). If we apply this passive rotation to the ‘oblique’ refraction, beds must already have an exceptional North-dipping attitude at time of the embryonic cleavage development in the competent sandstone.

Secondly, the competent layers in the North-dipping limb, which are interbedded in siltstone, show a cusped-lobate morphology (Fig. 9D). Such layer buckling in a

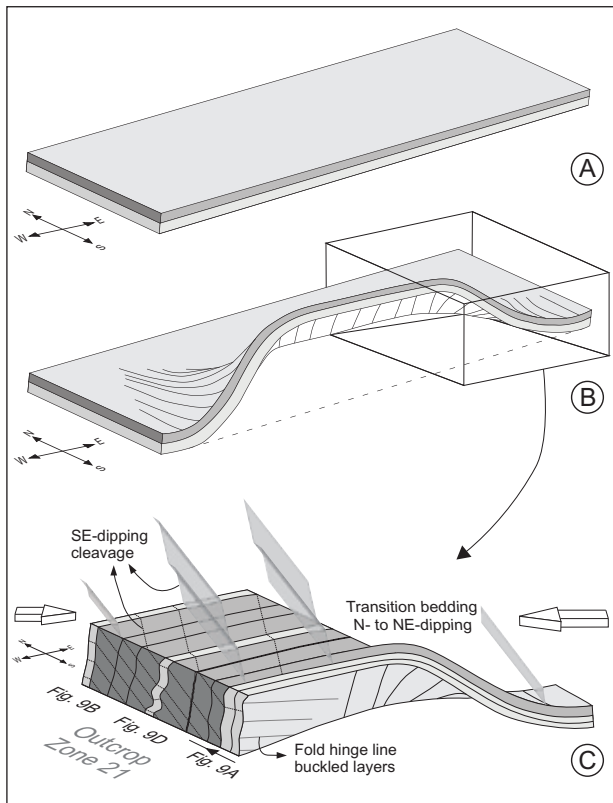


Figure 10: Evolutionary sketch of the North-dipping layers and their particular deformation structures in the Schwammenauel N section. Figure not to scale. A) Initial stage after sedimentation. B) Early tilting of the layers towards the North, with incipient development of the box fold. C) Progressive SE-NW directed Variscan shortening, as represented by a slaty cleavage, causes buckled layers in the box fold and oblique cleavage refraction across the competent beds. The slaty cleavage remains regionally axial planar. The formation of bedding-parallel veins predates phase B as they are also buckled in phase C.

single limb, however, is observed nowhere else in the study area, which indicates that this North-dipping attitude is rather exceptional in the area. The origin of this buckling can be unravelled by means of the orientation of the pervasive cleavage in the surrounding siltstone. Theoretically, cleavage is a result of the tectonic shortening in the incompetent units and will be oriented nearly perpendicular to the regional tectonic transport. In this North-dipping flank, cleavage is oriented at high angles to the buckled layers (Table 1 & Fig. 10C). Hence, at the time of pervasive cleavage development, the layers must already have been tilted towards the North, otherwise they would not start to buckle.

Thirdly, a divergent cleavage fanning is present near these small-scale folds. Cleavage seems to be squeezed in the cusps, whereas in the lobate parts cleavage diverges towards the cusps, indicating that cleavage development was closely related to the buckling of the layers. Moreover, also the fold hinges of these buckled folds (085/45) plunge in the same direction as the local bedding-cleavage intersection lineation (085/36).

These three arguments suggest that buckling and cleavage development were contemporaneous (Fig. 10C) and post-date an early tilting of the layers towards the North (Fig. 10B). Such a peculiar configuration of tilted beds could possibly develop during the incipient development of the periclinal folds, near the transition of a periclinal ending of a fold with the fold limb of an adjacent fold.

Finally, to give a conclusive answer to the relative timing of this early tilting, also the characteristics of the veins in the North-dipping layers have to be included. The layers comprise bedding-(sub)perpendicular veins, which have an early, burial origin (see 5.1.), as well as bedding-parallel quartz veins, which are formed by thrusting and also show a buckled morphology (see 5.2.). In other outcrops, however, bedding-parallel veins are usually planar (see 5.2. for characteristics). The latter observations indicate that tilting post-dates both veining events but presumably occurred before the main cleavage development and overall folding.

5. Veins

Contrary to the central HASB, where a single, well-arranged vein-set (Kenis, 2004) is present, rocks in the periphery are characterised by an abundance of different types of quartz veins. Two vein types can be recognised; quartz veins (1) (sub)perpendicular to bedding, common in and mostly confined to the competent sandstone beds (5.1.) and (2) parallel to bedding, at the interface of the competent and incompetent units, as well as interbedded in competent and incompetent sequences (5.2.). Furthermore also syntectonic quartz veins, which cannot be classified into (1) and (2), are observed (5.3.).

5.1. Bedding-(sub)perpendicular veins

A geometrical analysis of the quartz veins in the study area shows that the majority of veins are oriented at high angles to bedding, regardless of their orientation with respect to the folds. Vein dimensions vary considerably. Thickness ranges from millimetric, hairline-thin veins up to centimetre-thick composite veins (Fig. 11A & B), sometimes lensoid in shape (Fig. 11C). The thin hairline veins are mostly present in thin sandstone beds and are closely spaced. The thicker veins, on the other hand, are more widely spaced. Vein spacing shows a correlation to the layer thickness, although this correlation is not linear and does not correspond with the fracture spacing statistics of Price & Cosgrove (1990; p. 58).

Macroscopically, the composite veins show several pelitic host rock inclusions, which are more or less parallel to the vein wall. A composite vein can also comprise several smaller quartz veins, which initially grew separately but at the end formed one composite vein (Fig. 11E). Bedding-(sub)perpendicular veins are mostly limited to the coarse-grained competent sandstone layers. Veins restricted to a single bed, vary in shape from planar to curved (Fig. 11D). Furthermore, also slightly buckled veins are observed, sometimes cross-cutting planar veins

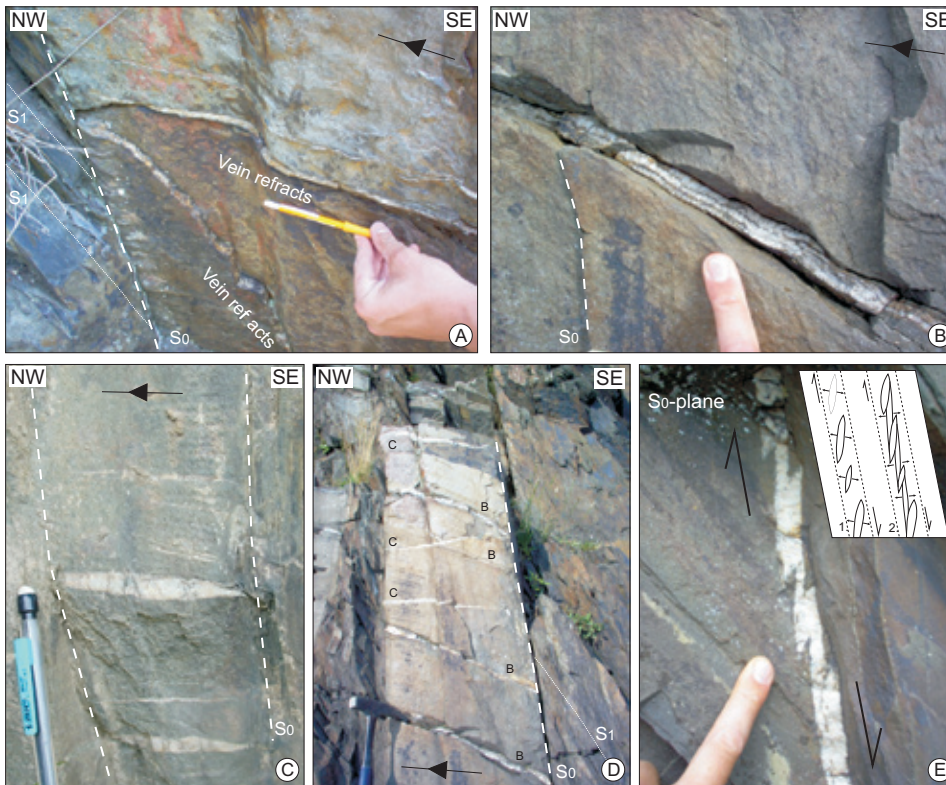


Figure 11 : Bedding-(sub)perpendicular vein characteristics. See Fig. 4 for location of zones. A) Vein refraction of two different vein generations at the competent-incompetent interface (m30, zone 3). B) A composite vein (generation B) which comprises several quartz laminae and thin host-rock inclusion bands (m360, zone 9). C) Lensoid quartz veins, subperpendicular to bedding (zone 18; Hubertus Höhe). D) Curved (generation B) and buckled (generation C) veins with mutual cross-cutting relationships. Cleavage refraction in between the veins is identical in orientation as that of the curved veins of generation B (m360, zone 9). E) An en-echelon sheared vein and model of vein formation based on the vein geometry (zone 18; Hubertus Höhe).

(Fig. 11D). If veins cross-cut multilayered sequences, they refract at the interface of a competent and an incompetent unit (Fig. 11A).

Observations on the bedding surface, hardly ever exposed, reveal that veins are rather limited in length, up to maximum a couple of metres. Bedding planes also show that veins can be displaced in an en-echelon arrangement, indicative for a shear perpendicular to the bedding (e.g. Fig. 11E). An overall shear sense has not been established; dextral (Fig. 11E) as well as sinistral shear has been observed on different veins with the same orientation. Beside quartz, these veins also contain chlorite, which are present at both vein walls. En-echelon veins internally show curved quartz fibres, in which the fibres are curved in a direction in agreement with the shear. Both features indicate an oblique vein opening with different amounts of shear during veining (see sketch on Fig. 11 E). Since these sheared veins have only been observed locally, implications of these observations are not clear yet.

In order to distinguish different vein generations, a considerable effort has been put in the orientation analysis of the veins. Based on cross-cutting relationships, different vein generations can be recognised (Fig. 12). Especially in the Wildenhof overturned limb (zone 9; Fig. 6), in which continuous outcrops are present, three distinct quartz vein generations are observed. The first and oldest generation A is only observed in a few sandstone beds and contains very thin, single opening veins. Generation B cross-cuts generation A and is widespread and very consistent in orientation (Figs 12A & B) along the entire Wildenhof overturned limb. This prominent generation B

mostly comprises composite (*i.e.* multiphased) veins with apparent host-rock inclusions (Fig. 11B), although single opening veins have also been observed. The veins are not always planar: also curved veins are present (Fig. 11D). Generation C is less consistent in orientation as generation B (Fig. 12A) and comprises sometimes slightly buckled veins without any host-rock inclusions. Generation C either cross-cuts generation B or varies in orientation in the vicinity of generation B, suggesting that already a competence contrast must have existed at time of veining of generation C. Locally, bedding-vein intersection lineation of generation B is oriented at a higher angle (45° - 70°) to the local bedding-cleavage intersection lineation than generation C (5° - 30°) (Fig. 12C).

In the competent beds along the normal SE-dipping limb (m112 and m190; zone 6), composite veins with similar characteristics as generation B are recognised. Their orientation is very consistent within a single outcrop (Fig. 12D). To evaluate if similar generations are present in the different fold limbs, both bedding of the gently SE-dipping layers at m112 and m190 (Fig. 12E) and bedding of the overturned limb at the campsite (Fig. 12B), are unfolded. This rotation is performed by firstly removing the effect of the plunging fold axis and afterwards unfolding the fold limbs towards the horizontal. Subsequent data shows that the veins in the normal limb (Fig. 12E) have a similar NE-SW strike as generation B in the overturned limb after unfolding (Fig. 12B) and that generation B thus seems to be consistent in trend. Zone 6 also shows different cross-cutting veins (e.g. Fig. 11A); unfolding exercises, however, do not give any satisfying results to compare these different cross-cuttings with

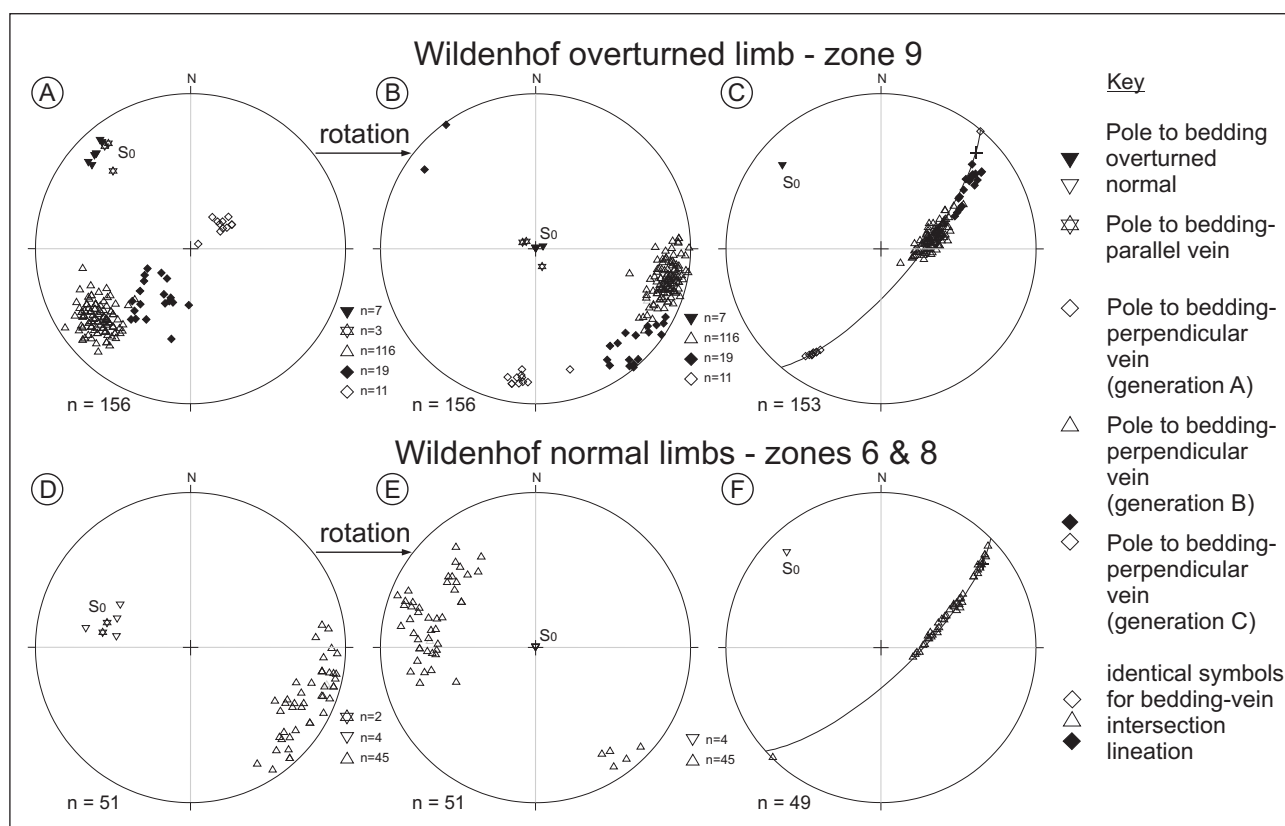


Figure 12 : A-B) Lower-hemisphere, equal-area projections of bedding-(sub)perpendicular veins along the Wildenhof section. Vein generations A, B & C in the Wildenhof overturned limb (zone 9) before (A) and after unfolding (B). C) Bedding-vein intersection lineation before unfolding. D-E) Veins in the normal limbs (zones 6 & 8) of the Wildenhof section before (D) and after unfolding (E). F) Bedding-vein intersection lineation before unfolding. See Fig. 4 for location of zones.

generations A and C at the Wildenhof campsite. These generations are thus not consistent along the Wildenhof cross-section. The latter suggests that, although the orientation of veins is consistent in orientation along one outcrop or along a fold, comparing different generations purely on the basis of the orientation of veins, along the whole Wildenhof cross-section, remains difficult.

5.2. Bedding-parallel veins

Two types of bedding-parallel veins (BPV) can be distinguished: (A) very thin (< 1 cm) single laminated veins and (B) thick (up to 10 cm) composite, laminated veins. Veins extend for several tens of metres, and aspect ratios are usually very high. The veins are present at the interface of beds of contrasting lithology (Fig. 13A), notably pelite and sandstone, as well as interbedded in incompetent and competent sequences. Bedding-parallel veins cross-cut (Fig. 13B) and offset (Fig. 13C) bedding-(sub)perpendicular veins (Fig. 13B), clearly indicating that both types of veining are separate events.

In outcrops where the sedimentary architecture shows an irregular pattern (*e.g.* point bars) thin bedding-parallel veins (A) are rather limited in length. The thick composite veins (B) have a complex internal fabric consisting of several distinct generations of quartz laminae intercalated with very thin, millimetric-size, pelitic wall-rock seams. Inclusion seams vary from very thin pelitic slices (Fig.

13D), approximately parallel to the vein walls, to brecciated pelitic host-rock fragments (Fig. 13E). This layering in composite veins suggests that fracturing and sealing are successive and recurrent processes during formation of the bedding-parallel veins (Séjourné *et al.*, 2005). No macroscopic observations (such as vein fibres) could reveal an opening trajectory. Furthermore, veins are folded and continue across fold hinges. The thickness of a composite vein is not constant but varies along the vein length. If a bedding-parallel vein is present in between pelites and overlying sandstone, the upper vein boundary has a flat morphology and the vein seems to be detached from the sandstone (Fig. 13F). On the contrary, veins usually show an intimate relationship (irregular boundary) with the underlying pelites. Locally, small veins are present in the underlying pelite and curve against the lower boundary of the bedding-parallel vein (Fig. 13G). Cleavage refracts across the small veins in the pelites. Both observations suggest that these small veins are local offshoots of the bedding-parallel veins and that they predate cleavage development.

The North-plunging box fold (Schwammenauel N section) contains layers which are buckled due to their abnormal orientation at the time of cleavage development (see 4.4.). Moreover, also bedding-parallel veins, interbedded in pelitic-silty sequences, as well as below and above sandstone beds, show a buckled nature and an



Figure 13: Bedding-parallel vein (BPV) characteristics. See Fig. 4 for location of zones. A) A thin flexural slip vein present at the contact of a competent and an incompetent unit (overturned limb; zone 13). The white arrow indicates the sense of displacement. B) Thin BPV cross-cutting a bedding-(sub)perpendicular vein (BppV) generation (m345, zone 9). C) Complex composite vein (BPV) offsetting a bedding-perpendicular vein (BppV) which continues through several beds (zone 12). D) Composite BPV interbedded in a pelitic sequence with thin pelitic inclusion seams parallel to bedding and vein wall (zone 18). E) Composite BPV including a host-rock fragment (see black arrow; m175, zone 8). F) Intimate relationship of a composite BPV with underlying pelite and detached from overlying sandstone (m175, zone 8). G) Small quartz veins overprinted by cleavage and in a close relationship with a composite bedding-parallel vein (m175, zone 8). H-I) Photograph (H) and illustrative sketch (I) of a buckled BPV in the North-dipping layers, showing the intimate relationship of the BPV with underlying pelite (zone 21). J) Composite BPV with different orientations of slickenlines (shown by black lines) on different quartz laminae (zone 21).

intimate relationship (irregular boundary) with the underlying pelites (Fig. 13H). This relationship is exemplified by small branches, branching off from the buckled composite bedding-parallel vein into the underlying pelites (Figs 13H & I). Cleavage abuts against the composite vein and seems to be squeezed into the cusps of the curved branch of the bedding-parallel vein (see detail on Fig. 13I). Veins are present in the cusps as well as in the lobate parts of the buckled sandstone layer (Fig. 9D).

Especially the composite bedding-parallel veins (B) are marked by slickenlines and slickenfibres. Slickenlines are uniform in trend on individual quartz laminae but differ slightly in orientation from lamina to lamina (Fig. 13J). Slickenlines are mostly at high angles to the bedding-cleavage intersection lineation, with the exception of those measured in the North-dipping layers in the Schwammenauel N section, where they are more or less parallel to the intersection. Distinct macroscopic shear sense indicators are not visible.

5.3. Syntectonic veins

In addition to bedding-(sub)perpendicular and -parallel veins, also minor tectonic structures with associated quartz veins are observed. Observations collectively suggest that these veins are related to overall buckling and thrusting.

Small-scale folds, such as folded layers at m5 and m185 in the Wildenhof section (Fig. 6), contain bedding-perpendicular hinge cracks filled up with quartz and tension gashes in the fold limbs. Tension gashes are oriented oblique to bedding and cross-cut bedding-(sub)perpendicular veins, indicating these gashes, which are formed due to folding of the layers, post-date the bedding-(sub)perpendicular veins. Such oblique tension gashes are most likely related to internal flexural flow of the layers during the formation of smaller-scale folds (cf. Fig. 21.12 in Ramsay & Huber, 1987).

Boudinaged layers occur only in outcrops in which cleavage is subparallel to bedding (m200, zone 8; zone 13). Interboudin veins, formed in the necks of the boudin layers, have only rarely been observed. Dilational jogs are observed in close relationship with bedding-(sub)parallel thrusts (m145, Wildenhof section). The origin of these jogs remains unclear; either they reflect pre-folding bedding-parallel thrusting (see further) and are in close relationship with the bedding-parallel veins, or they formed cogenetically with synbuckling to postbuckle thrusts such as the small-scale thrusts at m185 (see 4.2.1. and Fig. 7C).

6. Paragenesis

A detailed geometrical analysis of the characteristics of different vein types, combined with the analysis of features such as cleavage, folds and faults, allows us to set up a relative structural paragenesis in order to understand the structural evolution of the early veining in the periphery of the HASB (Fig. 14). A complex deformation history

was responsible for the formation of the different vein types.

6.1. Bedding-perpendicular veining

Bedding-perpendicular veining (Fig. 14B) definitely predates the Variscan fold-and-cleavage development. Cleavage cross-cuts the veins. Moreover, if a vein exceeds a competent bed into an incompetent unit, it is deformed and will refract along the competent-incompetent interface (Fig. 11A) in the same way as the cleavage does. The latter is indicative for pre-cleavage veining. Furthermore, unfolding reveals that both normal and overturned limbs in the Wildenhof section contain a similar vein generation B, which cross-cuts and is cross-cut by other generations, which are less consistent in orientation. Independent of the orientation of the beds, veins are oriented at high angles to bedding and remain bedding-(sub)perpendicular across fold hinges (see Fig. 6). The latter observations are indicative for pre-folding veining and suggest that veining occurred in a (sub)horizontal disposition, presumably still during burial. Unfolding also revealed that most veins are not perpendicular to bedding (Figs 12B & E). This implies that either veining did not occur perpendicular to bedding and hence that beds were already tilted at the time of veining or that veins were oriented initially perpendicular to bedding and afterwards were deformed into their subperpendicular attitude. An argument for the latter mechanism is the curved shape of the veins (Fig. 11D). Moreover, after the unfolding exercise, the veins in the normal limbs (Fig. 12E) dip in an opposite direction than the veins in the overturned limbs (Fig. 12B). This is in agreement with the change in orientation which is expected during flexural slip (Figs 11D & 14). It is thus likely that in the competent beds, the original planar veins were deformed during flexural slip folding. Remarkably, in some coarse grained-sandstone beds cleavage refraction has a similar curvature as the veins (Fig. 11D), corroborating the flexural slip deformation.

The composite nature of some of the veins (Fig. 11B) suggests that veins formed due to successive fracture and sealing phases through the structural evolution of the basin. Composite veins initially grew separately and became interconnected after successive phases (e.g. Hilgers & Urai, 2005).

6.2. Bedding-parallel veining

Based on bedding-parallel vein characteristics (5.2.), a relative chronology (Figs 14C) with respect to the bedding-(sub)perpendicular veins and the regional fold-and-cleavage development can be constrained. Bedding-parallel veins cross-cut, truncate and offset bedding-(sub)perpendicular veins, which implies that both types A and B post-date the bedding-(sub)perpendicular veins. The relative chronology with respect to fold-and-cleavage development is different for both types A and B.

The thin veins (A), on the one hand, are present at the lower contact of a sandstone bed with the underlying pelite. The latter configuration is the most favoured site

for flexural slip (Tanner, 1989). The displacement along the bedding planes is exemplified by slickenlines on the bedding-parallel veins which are, as observed, nearly orthogonal to the fold axis. Clear shear sense indicators with an opposite sense of displacement at both sides of a folds are, however, only locally visible (*e.g.* Fig. 13A). The absence of fibre steps makes it difficult to interpret all thin veins as flexural slip veins.

The composite veins (B), on the other hand, have a complex internal fabric and reflect a complex deformation history. The bedding-parallel veins in the North-plunging box fold (Figs 13D & H; zone 21) comprise several arguments to establish a relative chronology with respect to the main fold-and-cleavage development. Veins are present in the cusps as well as in the lobate parts of a buckled sandstone (Fig. 9D). Veins must thus have been simultaneously buckled with the sandstone. As argued in 4.4., buckling is related to cleavage development. Cleavage also abuts and diverges against the buckled vein. Both features suggest that the bedding-parallel veins existed before the cleavage developed and before the formation of the box fold.

Furthermore, composite veins continue across fold hinges without changing in thickness. The latter is incompatible with the mechanism of flexural slip, in

which bedding-parallel veins are absent across fold hinges (Tanner, 1989). Such a composite bedding-parallel vein continuing across a fold hinge, for example, is observed in the North-plunging box fold (Figs 8 & 10). Surprisingly, the slickenlines on this bedding-parallel vein in the North-dipping beds (zone 21) are, after unfolding, at a high angle (60°) to those in the NE-dipping beds (zone 22). This is in contrast to slickenlines on flexural slip veins, where they remain orthogonal to the fold axis at both sides of the fold (Tanner, 1989). The latter observations indicate that the composite bedding-parallel veins are not related to overall buckling, but instead predate the main fold-and-cleavage development. The different orientations of slickenlines on individual quartz laminae could reflect different stages of fracturing during which shear direction is not constant in orientation and cannot be explained by the formation of the box fold.

Bedding-parallel host-rock inclusion bands as well as bedding-parallel veins continuing across fold hinges have earlier been observed in the Rhenish Massif (de Roo *et al.*, 1992) and in the Oman mountains (Hilgers *et al.*, 2006a) where bedding-parallel shear is attributed to bedding-parallel vein formation. According to Passchier & Trouw (2005), BPVs play a role at initial stages of fold development rather than during flexural slip in maturing

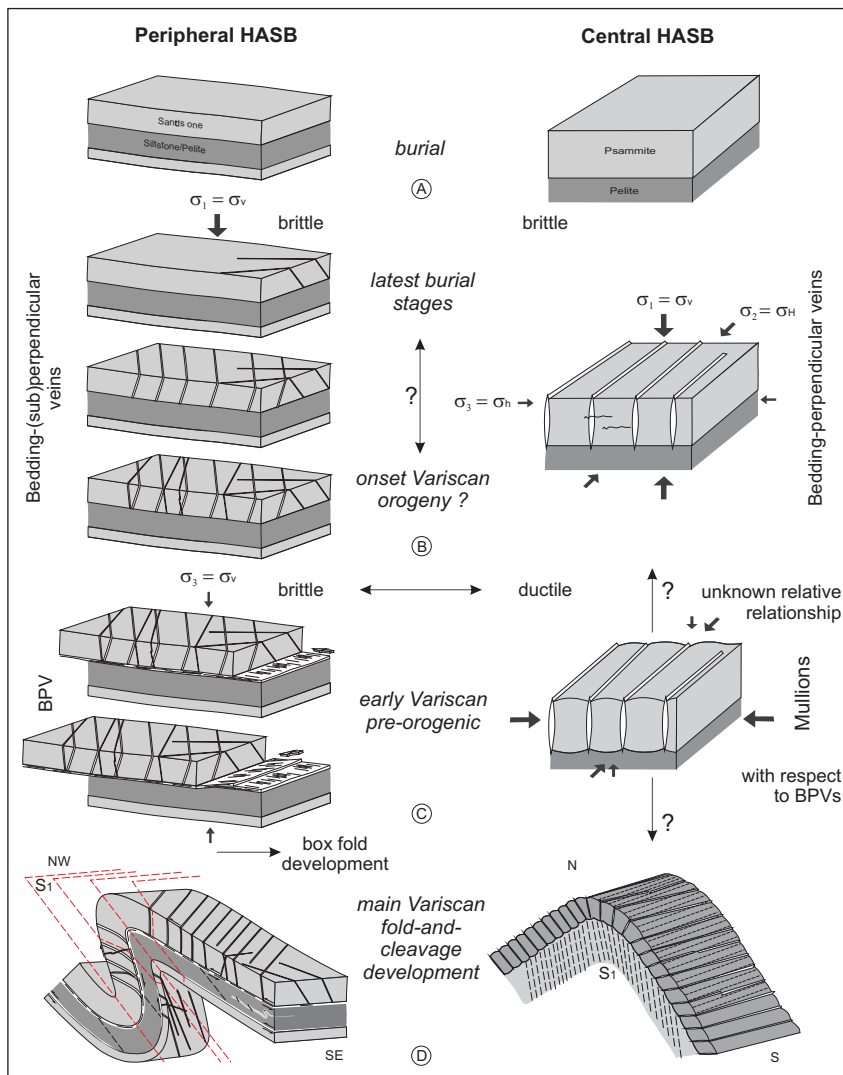


Figure 14: Comparison between the peripheral (this study) and central part (modified after Kenis, 2004) of the High-Ardenne slate belt. See text for discussion. A) Pragian to Lochkovian sedimentation. B) Differences in veining; the periphery is characterised by several generations of bedding-(sub)perpendicular veins, which are oriented differently, while the veins in the central part all belong to a well-arranged, parallel vein-set. Veining is considered to have occurred during the latest stages of the burial. C) Bedding-(sub)perpendicular veining is followed by bedding-parallel (BPV) veining in the periphery due to layer-parallel thrusting at the onset of Variscan shortening. Slickenlines reflect the different directions of thrusting. In the central part, the psammities deformed into mullions, below the brittle-ductile transition. Relative timing of both events is unclear. D) Subsequently during the main Variscan fold-and-cleavage development, both areas are deformed resulting in different, characteristic folds.

folds. Hence, bedding-parallel thrusting, which presumably took place during the early stages of the Variscan deformation, can be attributed to the development of type B veins. Incremental steps of thrusting are recorded by the accumulation of quartz laminae.

6.3. Synorogenic veining

Subsequently, as the tectonic deformation continues, overall buckling caused the characteristic NW-verging overturned folds with associated axial planar cleavage (Fig. 14D). Smaller-scale features with associated quartz veining such as interboudin veins, out-of-syncline fault-related veins, tension gashes, filled hinge cracks and thin bedding-parallel veins accompany folding. Due to flexural slip folding, bedding-(sub)perpendicular veins are displaced along the bedding contacts and/or are internally deformed.

6.4. Post-Variscan faults

Along the Wildenhof section several fault zones occur (4.2.). The occurrence of metre-scale pop-up structures and thrusts suggests that also the larger fault zones, with unknown displacements, could be thrust faults. According to Holland *et al.* (2006), however, the SE-dipping fault zone at m190 (Fig. 6) and comparable fault zones in the synclinal hinge at m220, are normal faults with a variable fault width. These authors describe these fault zones as a fault zones with a heterogeneous assemblage of strands of weakly to strongly deformed fault gouge and with differently deformed claystone material. They conclude from the thickness of the fault zone that the displacement is less than a few metres. An analysis of the clay gouge of the fault at m190 (Holland *et al.*, 2006) pointed out that the material is free of any minerals that could indicate a deep burial as would be expected under the conditions of the Variscan Orogeny. Moreover, the porosity of the clay gouge is much higher than the “overconsolidated” host rocks (*i.e.* pelites). Therefore Holland *et al.* (2006) suggested that deformation must have taken place in much shallower conditions than that during the Variscan deformation.

7. Discussion

7.1. Stress field related to bedding-(sub)perpendicular veins

We have shown that, although veins locally seem to be consistent in orientation, correlation of different vein generations in between fold limbs remains difficult. Nevertheless, one single consistent vein generation (generation B) could be recognised which cross-cuts or is cross-cut by other veins (*e.g.* generation A & C; Wildenhof section). Above arguments suggest that fracturing and veining, regardless of the vein filling mechanism, must have occurred in different phases and predate overall folding.

Macro- and preliminary microstructural observations indicate that these veins can be recognised as extension veins that opened in incremental steps, suggesting a crack-seal (Ramsay, 1980) mechanism (see also Hilgers *et al.*, 2006b). Assuming that bedding-(sub)perpendicular veins formed early, we should be able to estimate the direction of the principal stresses at the time of veining. Crack-seal veins form perpendicular to the least principal stress (σ_3). Since these veins formed in a (sub)horizontal bedding disposition, veins were unfolded (Figs 12B & E), in order to determine the least principal stress direction (σ_3). Results of this unfolding show a NNE-SSW to NE-SW orientation for the veins. This implies a WNW-ESE direction for the least principal stress (σ_3). This, however, has to be handled with caution. Due to the different cross-cutting relationships, and due to the non-consistent orientation of some generations, it is not certain if all vein generations formed in the same stress conditions. After all, generation A (Fig. 12B) is oriented East-West and is nearly perpendicular to generations B and C.

7.2. Bedding-parallel veins

The formation of bedding-parallel veins (BPV) has caused considerable debate. Most authors agree that these veins usually form in basins with alternating beds, in which layer-parallel slip, either due to folding or to thrusting, can easily occur. The principal issue is whether the veins developed before (*e.g.* Fitches *et al.*, 1986), at the onset (*e.g.* Cosgrove, 1993; Hilgers *et al.*, 2006a) or during (*e.g.* Tanner, 1989) folding. It does not lie in the scope of this paper to review all possible mechanisms on the formation of bedding-parallel veins, neither to solve the question on the formation of bedding-parallel veins in general. Some models seem applicable to the veins observed in the Rursee area and are quoted in the discussion. The reader is referred to Fowler (1996), Séjourné *et al.* (2005) and Hilgers *et al.* (2006a) for further reading on the origin of bedding-parallel veins.

The controversy about distinguishing pre- from syn-folding BPVs is similar to that of other pre- versus syn-deformational structures (*e.g.* distinguishing pre- from syntectonic folds). Pre- and syn-folding BPVs share common characteristics (Fowler & Winsor, 1997) such as multiple quartz laminae separated by thin pelitic inclusion seams, *i.e.* composite or laminated veins, as well as slickenlines with varying orientation on individual laminae. Both observations can be explained by flexural slip (Tanner, 1989; Fowler & Winsor, 1997) or by thrusting (Jessell *et al.*, 1994; Koehn & Passchier, 2000). Furthermore, the quartz laminae in the laminated veins suggest that opening and sealing of the veins are successive and recurrent features (Séjourné *et al.*, 2005). Also the thickness of laminated veins has been correlated with the net slip along the veins. Flexural slip veins are usually thin veins while, on the other hand, sheared veins may change in thickness up to several tens of centimetres (Fowler & Winsor, 1997). These common features make it difficult to separate pre- from syn-folding bedding-parallel veins. Moreover, the possibility exists that both models

are mutually not exclusive. A continuous evolution of pre-folding into flexural slip syn-folding veins may exist (Tanner, 1990).

In order to distinguish pre- from syn-folding veins, their microstructures should be analysed. In flexural-slip veins, on the one hand, small crystal fibres reflect the opening trajectory of the veins and the step-like shear fibre steps are directed to the fold hinges (Tanner, 1989). On the other hand, BPVs formed by bedding-parallel thrusting, are characterised by small, bedding-(sub)parallel inclusion trails and crack-seal bands, which both track the opening direction during vein formation and reflect the amount of displacement of sedimentary layers during layer-parallel slip (for different mechanisms see Jessell *et al.*, 1994; Koehn & Passchier, 2000). Although a lot of models concerning the origin of BPVs are based on the original microstructures, progressive deformation partly destroys the original fabric, which it will make hard to determine the origin of veining purely based on the microstructures.

Different configurations on the occurrence of the BPVs to the surrounding rocks have been observed. In the Rhenish Massif, BPVs tend to occur in slates near boundaries between rocks of contrasting competence (de Roo & Weber, 1992). Fitches *et al.* (1986) note that pre-folding BPVs, which formed by the process of hydraulic jacking, mainly occur in homogeneous pelite or at the upper contact of a sandstone bed with overlying pelite. In contrast, the most favoured site of flexural slip veins is the lower contact of a sandstone bed with the underlying slate (Tanner, 1989; Fowler & Winsor, 1997). Despite these findings, we found no systematic relationship between the occurrence of the composite BPVs and hosting lithologies in the Rursee area. Laminated veins either occur interbedded in a sequence (Fig. 13D) or near the pelite-sandstone interface (Fig. 13F; see 5.2.1.).

7.3. Comparison periphery-central HASB (Fig. 14)

In the central part of the HASB, exposing the deepest part of the basin (highest degree of burial metamorphism), the occurrence of a regular and consistent set of bedding-perpendicular veins suggests that veining occurred in a highly anisotropic stress field. Veins, which formed in the presence of high fluid pressures, were orientated originally NE to NNE and hence reflect a WNW-ESE to NW-SE directed least principal stress (σ_3) at the time of veining (Kenis, 2004). In the periphery of the slate belt, exposing higher levels of the basin (lower degree of burial-related metamorphism), the structural control on the veins is less obvious. The different cross-cutting vein generations suggest that fracturing/veining occurred in a less anisotropic stress field than in the central part of the basin and that the stress field cannot clearly be defined by a macrostructural analysis. Whether veining occurred simultaneously in both areas remains unclear and needs further research.

Subsequently, the onset of the Variscan shortening is expressed differently in both areas. In the deeper parts of the basin, below the brittle-ductile transition, psammites

deformed ductilely into mullions, pinned in between lensoid quartz veins (Kenis, 2004). Towards the periphery of the slate belt mullions are absent and shortening is exemplified by bedding-parallel quartz veins, during which the least principal stress (σ_3) was vertical. Also the relative timing of the mullions with respect to the BPVs in the periphery is still a matter of discussion.

8. Conclusions & perspectives

We demonstrated that bedding-(sub)perpendicular quartz veins originated from early brittle fracturing, probably during burial stages. Extensional crack-seal veins exemplify that fracturing and veining were successive and recurrent and occurred in a less anisotropic stress field than in the central part of the basin.

Furthermore, two types of bedding-parallel veins, *i.e.* thin veins (A) and composite veins (B), can be recognised. The thin veins (A) result from bedding-parallel slip during flexural slip folding while the composite bedding-parallel veins (B) are thought to be due to bedding-parallel thrusting prior to folding. We have to keep in mind, however, that type B veins may be reactivated during flexural slip folding. Evidence of thrusting includes: i) BPVs are folded and continuously present across fold hinges (cf. Cosgrove, 1993, 1995); ii) the extreme variability of slip orientations in a single BPV, varying from orthogonal to parallel to the local fold hinge line, indicated that laminated veins formed during recurrent and successive slip (cf. Fitches *et al.*, 1986; Fowler & Winsor, 1997); iii) small-scale buckled veins concomitant with buckle folds within the North-dipping limb of the box fold show that the veins predate the main fold-and-cleavage development (cf. de Roo & Weber, 1992; Cosgrove, 1995); iv) cleavage fans out against buckled BVPs and overprints the straight veins (cf. Fowler & Winsor, 1997).

Macroscopic observations, either on outcrop- or hand-scale, can only reveal the relative spatial and temporal relationship of the veins with respect to minor structures and fold-and-cleavage development. The veining mechanism remains an open question. Further research will firstly focus upon a microstructural analysis of vein microstructures in order to reveal the veining mechanism and the subsequent deformation. Secondly, as orientation data of the veins do not reveal the structural evolution of the different vein generations, further research efforts will concentrate on the microthermometry of the primary fluid inclusion of vein quartz. This research strategy will allow us to compare different stress paths and veining conditions between the central and peripheral parts of the High-Ardenne slate belt, eventually enabling to reconstruct the regional fluid system and stress field evolution in an overpressured basin at the beginning of an orogeny. Thirdly, also oxygen isotopes of the quartz veins and adjacent host rock will be examined in order to check if veining occurred in thermal and geochemical equilibrium with the host rock.

Acknowledgements

We would like to acknowledge reviewers Jacques L. R. Touret and Timothy N. Debacker for their helpful and constructive remarks, which led to shortening of the paper. We also thank Jean-Clair Duchesne for editing the manuscript. This paper frames in the research project KAN 1.5.128.05 of the Fonds voor Wetenschappelijk Onderzoek – Vlaanderen. Manuel Sintubin is a Research Associate of the Bijzonder Onderzoeksfonds at the K.U.Leuven. This study has also benefited from discussions at the RWTH.

References

- COSGROVE, J.W., 1993. The interplay between fluids, folds and thrusts during the deformation of a sedimentary succession. *Journal of Structural Geology*, 15(3-5): 491-500.
- COSGROVE, J.W., 1995. The interplay between fluids, folds and thrusts during the deformation of a sedimentary succession: Discussion. *Journal of Structural Geology*, 10: 1478-1480.
- DE ROO, J.A. & WEBER, K., 1992. Laminated veins and hydrothermal breccia as markers of low-angle faulting, Rhenish Massif, Germany. *Tectonophysics*, 208: 413-430.
- DITTMAR, D., MEYER, W., ONCKEN, O., SCHIEVENBUSCH, T., WALTER, R. & VON WINTERFELD, C., 1994. Strain partitioning across a fold and thrust belt: the Rhenish Massif, Mid-European Variscides. *Journal of Structural Geology*, 16(10): 1335-1352.
- FIELITZ, W., 1992. Variscan transpressive inversion in the northwestern central Rhenohercynian belt of western Germany. *Journal of Structural Geology*, 14(5): 547-563.
- FIELITZ, W. & MANSY, J.-L., 1999. Pre- and synorogenic burial metamorphism in the Ardenne and neighbouring areas (Rhenohercynian zone, central European Variscides). In Sintubin, M., Vandycke, S. & Camelbeeck, T. (eds.), *Palaeozoic to Recent tectonics in the NW European Variscan Front Zone*. *Tectonophysics*, 309: 227-256.
- FITCHES, W.R., CAVE, R., CRAIG, J. & MALTMAN, A.J., 1986. Early veins as evidence of detachment in the Lower Palaeozoic rocks of the Welsh Basin. *Journal of Structural Geology*, 8(6): 607-620.
- FOWLER, T.J., 1996. Flexural-slip generated bedding-parallel veins from central Victoria, Australia. *Journal of Structural Geology*, 18(12): 1399-1415.
- FOWLER, T.J. & WINSOR, C.N., 1997. Characteristics and occurrence of bedding-parallel slip surfaces and laminated veins in chevron folds from the Bendigo-Castlemaine goldfields: implications for flexural-slip folding. *Journal of Structural Geology*, 19(6): 799-815.
- GARCIA-CASTELLANOS, D., CLOETINGH, S. & VAN BALEN, R., 2000. Modelling the Middle Pleistocene uplift in the Ardennes-Rhenish Massif: thermo-mechanical weakening under the Eifel? *Global and Planetary Change*, 27: 39-52.
- GOEMAERE, E. & DEJONGHE, L., 2005. Palaeoenvironmental reconstruction of the Mirwart Formation (Pragian) in the Lambert quarry (Flamierge, Ardenne, Belgium). *Geologica Belgica*, 8(3): 37-52.
- HANCE, L., GHYSEL, P., LALOUX, M., DEJONGHE, L. & MANSY, J.-L., 1999. Influence of a heterogeneous lithostructural layering on orogenic deformation of the Variscan Front Zone (eastern Belgium). In Sintubin, M., Vandycke, S. & Camelbeeck, T. (Editors), *Palaeozoic to Recent tectonics in the NW European Variscan Front Zone*. *Tectonophysics*, 309: 161-177.
- HILGERS, C., BÜCKER, C. & URAI, J.L., 2006b. Fossil overpressures compartments? A case study from the Eifel area and some general aspects. In: *11. Symposium „Tektonik, Struktur- und Kristallingeologie“* (edited by Philipp, S., Leiss, B., Vollbrecht, A., Tanner, D. & Gudmundsson, A.). Universitätsdrucke Göttingen, Göttingen, Germany, 87-89.
- HILGERS, C., BÜCKER, C., URAI, J.L., LITKE, R., POST, A., VAN DER ZEE, W. & KRAUS, J., 2000. Field study of an exhumed lower Devonian high pressure reservoir. *Geophysical Research Abstracts*, 2(SE34): 47.
- HILGERS, C., KIRSCHNER, D.L., BRETON, J.-P. & URAI, J.L., 2006a. Fracture sealing and fluid overpressures in limestones of the Jabal Akhdar dome, Oman mountains. *Geofluids*, 6: 168-184.
- HILGERS, C. & URAI, J.L., 2002. Microstructural observations on natural syntectonic fibrous veins: implications for the growth process. *Tectonophysics*, 352: 257-274.
- HILGERS, C. & URAI, J.L., 2005. On the arrangement of solid inclusions in fibrous veins and the role of the crack-seal mechanism. *Journal of Structural Geology*, 27: 481-494.
- HOFFMANN, K., 1961. Die Tektonik am Südrand des Hohen Venns. *Neues Jahrbuch für Geologie und Paläontologie, Abhandlungen*, 111: 341-367.
- HOLLAND, M., URAI, J.L., VAN DER ZEE, W., STANJEK, H. & KONSTANTY, J., 2006. Fault gouge evolution in highly overconsolidated claystones. *Journal of Structural Geology*, 28: 323-332.
- JESSELL, M.W., WILLMAN, C.E. & GRAY, D.R., 1994. Bedding parallel veins and their relationship to folding. *Journal of Structural Geology*, 16(6): 753-767.
- KENIS, I., 2004. *Brittle-Ductile Deformation Behaviour in the Middle Crust as Exemplified by Mullions (Former “Boudins”) in the High-Ardenne Slate Belt, Belgium*. Aardkundige Mededelingen, 14. Leuven University Press, Leuven.
- KENIS, I. & SINTUBIN, M., 2007. About boudins and mullions in the Ardenne-Eifel area (Belgium, Germany). *Geologica Belgica*, 10(1-2): 79-91.

- KENIS, I., SINTUBIN, M., MUCHEZ, P. & BURKE, E.A.J., 2002. The "boudinage" question in the High-Ardenne Slate Belt (Belgium): a combined structural and fluid-inclusion approach. *Tectonophysics*, 348: 93-110.
- KNAPP, G., 1980. Erläuterungen zur Geologischen Karte der nördlichen Eifel 1 : 100 000, Krefeld.
- KOEHN, D. & PASSCHIER, C.W., 2000. Shear sense indicators in striped bedding-veins. *Journal of Structural Geology*, 22: 1141-1151.
- LACQUEMENT, F., 2001. *L'Ardenne Varisque. Déformation progressive d'un prisme sédimentaire pré-structuré, de l'affleurement au modèle de chaîne*. Publication. Société Géologique du Nord, Lille.
- MANSY, J.-L. & LACQUEMENT, F., 2003. Le Paléozoïque du Nord de la France et de la Belgique. *Géologues*, 133-134: 7-24.
- MEILLIEZ, F. & MANSY, J.-L., 1990. Déformation pelliculaire différenciée dans une série lithologique hétérogène: le Dévon-Carbonifère de l'Ardenne. *Bulletin de la Société géologique de France*, (8), VI(1): 177-188.
- ONCKEN, O., VON WINTERFELD, C. & DITTMAR, U., 1999. Accretion of a rifted passive margin: The Late Paleozoic Rhenohercynian fold and thrust belt (Middle European Variscides). *Tectonics*, 18(1): 75-91.
- PASSCHIER, C.W. & TROUW, R.A.J., 2005. Dilatation Sites - Veins, Strain Shadows, Fringes and Boudins. In Passchier, C.W. & Trouw, R.A.J. (eds.), *Microtectonics*. Springer - Verlag, Berlin: 159-187.
- PILGER, A. & SCHMIDT, W., 1957. Die Mullion-Strukturen in der Nord-Eifel. *Abhandlungen Hessischen Landesamtes für Bodenforschung*, 20: 1-53.
- PRICE, N.J. & COSGROVE, J.W., 1990. *Analysis of geological structures*. Cambridge University Press, Cambridge.
- RAMSAY, J.G., 1980. The crack-seal mechanism of rock deformation. *Nature*, 284: 135-139.
- RAMSAY, J.G. & HUBER, M.I., 1987. *The techniques of modern structural geology. Volume 2: folds and fractures*. Academic Press, London.
- RIBBERT, K.-H., 1992. Erläuterungen zu Blatt C5502 Aachen. Geologisches Landesamt Nordrhein-Westfalen, Krefeld.
- RICHTER, D., 1967. Aachen und Umgebung: Nordeifel und Umgebung. *Sammlung geologischer Führer*, 48.
- SÉJOURNÉ, S., MALO, M., SAVARD, M.M. & KIRKWOOD, D., 2005. Multiple origin and regional significance of bedding parallel veins in a fold and thrust belt: The example of a carbonate slice along the Appalachian structural front. *Tectonophysics*, 407: 189-209.
- SCHULTZ, B., AUDREN, C. & TRIBOULET, C., 2002. Oxygen isotope record of fluid-rock-SiO₂ interaction during Variscan progressive deformation and quartz veining in the meta-volcanosediments of Belle-Ile (Southern Brittany). *Journal of Structural Geology* 24, 1281-1297.
- SIPPLI, G., 1981. Ausbildung und Verbreitung von K-Boudins (Mullions) in der westlichen Nordeifel und Überlegungen zu ihrer Entstehung. Unpublished Diplom Thesis, RWTH Aachen.
- SPAETH, G., 1979. Neuere Beobachtungen und Vorstellungen zur Variszischen Tektonik der westlichen Nordeifel (Rheinisches Schiefergebirge). *Zeitung der Deutschen Geologischen Gesellschaft*, 130: 107-121.
- SPAETH, G., 1986. Boudins und Mullions in devonischen Schichtfolgen der Nordeifel und Ardennen; Erscheinungsbild, Entstehung und Umformung. *Nachrichten - Deutsche Geologische Gesellschaft*, 35: 74-75.
- TANNER, G.P.W., 1989. The flexural-slip mechanism. *Journal of Structural Geology*, 11(6): 635-655.
- TANNER, G.P.W., 1990. The flexural-slip mechanism: Reply. *Journal of Structural Geology*, 12(8): 1085-1087.
- TREAGUS, S.H., 1983. A theory of finite strain variation through contrasting layers, and its bearing on cleavage refraction. *Journal of Structural Geology*, 5: 351-368.
- URAI, J.L., WILLIAMS, P.F. & VAN ROERMOND, H.L.M., 1991. Kinematics of crystal growth in syntectonic fibrous veins. *Journal of Structural Geology*, 13(7): 823-836.
- URAI, J.L., SPAETH, G., VAN DER ZEE, W. & HILGERS, C., 2001. Evolution of Mullion (formerly Boudin) structures in the Variscan of the Ardennes and Eifel. *Journal of the Virtual Explorer*, 3: 1-15.
- VAN BAELEN, H. & SINTUBIN, M., 2008. Kinematic consequences of an angular unconformity in simple shear: An example from the southern border of the Lower Palaeozoic Rocroi inlier (Naux, France). *Bulletin de la Société géologique de France*, 179(1): 73-87.
- VON WINTERFELD, C.-H., 1994. *Variszische Deckentektonik und devonische Beckengeometrie der Nord-Eifel - Ein quantitatives Modell (Profilbilanzierung und Strain-Analyse im Linksrheinischen Schiefergebirge)*. Aachener Geowissenschaftliche Beiträge. Verlag der Augustinus Buchhandlung, Aachen.
- WALTER, R., 1992. *Geologie von Mitteleuropa*. E. Schweizerbart'sche Verlagsbuchhandlung, Stuttgart.
- WÜNSTORF, W., 1931. Über das Unterdevon auf dem Südflügel des Venn-Sattels. *Sitzung Berliner Preußische geologische Landesanstalt*, 6: 157-168.
- WÜNSTORF, W., 1934. Bericht über die Exkursion durch das Cambrium, Silur und Unterdevon auf den Südflügel des Venns-Sattels am 22 und 23 mai 1932. Verhandlung des naturhistorischen Vereins der preussischen Rheinlande und Westfalens, 91: 112-119.
- WÜNSTORF, W., 1936. Bericht über die Begehung des Unterdevons der Nordeifel. *Jahrbuch preußische geologische Landesanstalt*, 56: 326-329.
- WÜNSTORF, W., 1943. Erläuterungen zu den Blättern 5303 Rötgen - Eupen, 5304 Nideggen. Geologische Karte Deutsches Reich, Berlin, 76 p.